

# Pyrazolyl Derivatives as Bifunctional Chelators for Labeling Tumor-Seeking Peptides with the *fac*-[M(CO)<sub>3</sub>]<sup>+</sup> Moiety (M = <sup>99m</sup>Tc, Re): Synthesis, Characterization, and Biological Behavior

Susana Alves,<sup>†</sup> António Paulo,<sup>†</sup> João D. G. Correia,<sup>†</sup> Lurdes Gano,<sup>†</sup> Charles J. Smith,<sup>‡</sup> Timothy J. Hoffman,<sup>‡</sup> and Isabel Santos<sup>\*,†</sup>

Departamento de Química, ITN, Estrada Nacional 10, 2686-953 Sacavém Codex, Portugal, The Harry S. Truman Memorial Veterans' Hospital, Columbia, Missouri 65201, Department of Radiology and Department of Internal Medicine, University of Missouri–Columbia School of Medicine, Columbia, Missouri 65211, and University of Missouri–Columbia Research Reactor Center, Columbia, Missouri 65211. Received August 26, 2004; Revised Manuscript Received January 6, 2005

Radiolabeling of biologically active molecules with the [<sup>99m</sup>Tc(CO)<sub>3</sub>]<sup>+</sup> unit has been of primary interest in recent years. With this in mind, we herein report symmetric (**L**<sup>1</sup>) and asymmetric (**L**<sup>2</sup>–**L**<sup>5</sup>) pyrazolyl-containing chelators that have been evaluated in radiochemical reactions with the synthon [<sup>99m</sup>Tc(H<sub>2</sub>O)<sub>3</sub>(CO)<sub>3</sub>]<sup>+</sup> (**1a**). These reactions yielded the radioactive building blocks [<sup>99m</sup>Tc(CO)<sub>3</sub>(κ<sup>3</sup>-L)]<sup>+</sup> (L = **L**<sup>1</sup>–**L**<sup>5</sup>, **2a**–**6a**), which were identified by RP-HPLC. The corresponding Re surrogates (**2**–**6**) allowed for macroscopic identification of the radiochemical conjugates. Complexes **2a**–**6a**, with log *P*<sub>o/w</sub> values ranging from –2.35 to 0.87, were obtained in yields of ≥90% using ligand concentrations in the 10<sup>–5</sup>–10<sup>–4</sup> M range. Challenge studies with cysteine and histidine revealed high stability for all of these radioactive complexes, and biodistribution studies in mice indicated a fast rate of blood clearance and high rate of total radioactivity excretion, occurring primarily through the renal-urinary pathway. Based on the framework of the asymmetric chelators, the novel bifunctional ligands 3,5-Me<sub>2</sub>-pz(CH<sub>2</sub>)<sub>2</sub>N((CH<sub>2</sub>)<sub>3</sub>COOH)(CH<sub>2</sub>)<sub>2</sub>NH<sub>2</sub> (**L**<sup>6</sup>) and pz(CH<sub>2</sub>)<sub>2</sub>N((CH<sub>2</sub>)<sub>3</sub>COOH)(CH<sub>2</sub>)<sub>2</sub>NH<sub>2</sub> (**L**<sup>7</sup>) have been synthesized and their coordination chemistry toward (NEt<sub>4</sub>)<sub>2</sub>[ReBr<sub>3</sub>(CO)<sub>3</sub>] (**1**) has been explored. The resulting complexes, *fac*-[Re(CO)<sub>3</sub>(κ<sup>3</sup>-L)]Br (**L**<sup>6</sup> (**7**), **L**<sup>7</sup> (**8**)), contain tridentate ancillary ligands that are coordinated to the metal center through the pyrazolyl and amine nitrogen atoms, as observed for the other related building blocks. **L**<sup>6</sup> and **L**<sup>7</sup> were coupled to a glycyglycine ethyl ester dipeptide, and the resulting functionalized ligands were used to prepare the model complexes *fac*-[Re(CO)<sub>3</sub>(κ<sup>3</sup>-3,5-Me<sub>2</sub>-pz(CH<sub>2</sub>)<sub>2</sub>N(glygly)(CH<sub>2</sub>)<sub>2</sub>NH<sub>2</sub>)]<sup>+</sup> (**9/9a**) and *fac*-[Re(CO)<sub>3</sub>(κ<sup>3</sup>-pz(CH<sub>2</sub>)<sub>2</sub>N(CH<sub>2</sub>)<sub>3</sub>(glygly)(CH<sub>2</sub>)<sub>2</sub>NH<sub>2</sub>)]<sup>+</sup> (**10/10a**) (M = Re, <sup>99m</sup>Tc). These small conjugates have been fully characterized and are reported herein. On the basis of the in vitro/in vivo behavior of the model complexes (**2a**–**6a**, **9a**, **10a**), we chose to evaluate the in vitro/in vivo biological behavior of a new tumor-seeking Bombesin pyrazolyl conjugate, [**L**<sup>6</sup>]-G-G-G-Q-W-A-V-G-H-L-M-NH<sub>2</sub>, that has been labeled with the [<sup>99m</sup>Tc(CO)<sub>3</sub>]<sup>+</sup> metal fragment. Stability, in vitro cell binding assays, and pharmacokinetics studies in normal mice are reported herein.

## INTRODUCTION

The most recent approaches for radiopharmaceutical development are mainly based on the search for target-specific radiopharmaceuticals (**1**–**4**). This strategy involves the labeling of biologically relevant molecules, somehow related to a certain disease or disease type, and intends to improve the specificity of diagnosis and therapy in nuclear medicine (**1**–**4**).

Most of the hormonal messengers are peptides, which are involved in more fundamental biological processes than any other class of molecules, including the regulation of cellular growth and proliferation in normal as well as in tumor cells (**4**–**7**). Moreover, most tumor cells overexpress receptors for regulatory peptides, which are

often specific for a certain tumor type (**5**–**7**). Many peptide receptors have already been identified and associated with a specific tumor type, stressing the interest in radiolabeling regulatory peptide analogues. Furthermore, the success obtained with the labeling of some of these peptides, such as somatostatin analogues, has encouraged further work in this field (**5**–**8**).

A recently introduced organometallic aquaion *fac*-[M(CO)<sub>3</sub>(H<sub>2</sub>O)<sub>3</sub>]<sup>+</sup>, M = Re, <sup>99/99m</sup>Tc, has opened new perspectives for the labeling of different biomolecules (**9**–**11**). The attractiveness of this low-valent precursor results from its particularly high thermodynamic stability, that is, high substitution stability of CO ligands and substitution lability of water molecules, which can be easily replaced by a variety of mono, bis, and tridentate ligands of different size, shape, and donor atom sets (**12**–**19**). This versatility allows for the synthesis of different building blocks with physicochemical properties matched to the biologically relevant molecule.

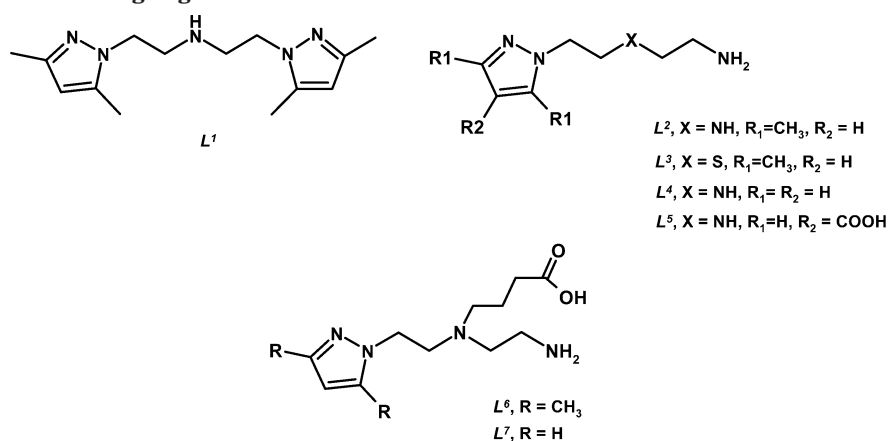
As part of our ongoing work on the search for bifunctional chelators suitable for the labeling of peptides with

\* To whom correspondence should be addressed. Telephone: 351-21-994 6201. E-mail: isantos@itn.mces.pt.

<sup>†</sup> ITN.

<sup>‡</sup> The Harry S. Truman Memorial Veterans' Hospital, University of Missouri–Columbia School of Medicine, and University of Missouri–Columbia Research Reactor Center.

## Chart 1. Pyrazolyl-Containing Ligands



the *fac*-[<sup>99m</sup>Tc(CO)<sub>3</sub>]<sup>+</sup> moiety, we have previously synthesized a family of asymmetric and symmetric pyrazolyl-containing ligands (**L**<sup>1</sup>–**L**<sup>3</sup> and **L**<sup>5</sup>) (Chart 1) and explored their chemistry with the precursor (NEt<sub>4</sub>)<sub>2</sub>[ReBr<sub>3</sub>(CO)<sub>3</sub>] (**1**). This has led to the synthesis of different building blocks of the type *fac*-[Re(CO)<sub>3</sub>(k<sup>3</sup>-L)]<sup>+</sup> (**20**–**22**).

As part of a study to select the most promising pyrazolyl-based chelators for further application on the labeling of biologically active peptides, we report herein on the synthesis, characterization, and biological evaluation of the corresponding <sup>99m</sup>Tc-building blocks, *fac*-[<sup>99m</sup>Tc(CO)<sub>3</sub>(k<sup>3</sup>-L)]<sup>+</sup>. These complexes have been obtained by reaction of the *fac*-[<sup>99m</sup>Tc(H<sub>2</sub>O)<sub>3</sub>(CO)<sub>3</sub>]<sup>+</sup> precursor with **L**<sup>1</sup>–**L**<sup>5</sup>. Taking advantage of the versatility of these systems, we also describe the synthesis and characterization of the novel bifunctional pyrazolyl-based chelators **L**<sup>6</sup> and **L**<sup>7</sup> (Chart 1), as well as the synthesis and characterization of the respective tricarbonyl rhenium complexes. The utility of the new ligand frameworks **L**<sup>6</sup> and **L**<sup>7</sup> is further demonstrated herein by radiolabeling and biological evaluation of [(**L**<sup>6</sup>)-G-G-G-Q-W-A-V-G-H-L-M-NH<sub>2</sub>], a GRPr specific analogue with tumor-targeting capability.

Bombesin (BBN) is a 14 amino acid peptide with very high affinity for the gastrin-releasing peptide receptor (GRPr). The function and in vivo distribution of the GRPr has been well established, showing expression in the central nervous system (CNS) and in peripheral tissues such as the pancreas or intestinal tract (**23**–**28**). The GRPr is also expressed on a variety of tumors including breast, prostate, pancreatic, and small-cell lung cancer (**23**–**28**). Therefore, radiolabeled BBN/GRP analogues such as [(**L**<sup>6</sup>)-G-G-G-Q-W-A-V-G-H-L-M-NH<sub>2</sub>] hold some potential to be used as site-directed diagnostic and/or therapeutic targeting motifs when radiolabeled with the appropriate radionuclide.

## MATERIALS AND METHODS

All chemicals and solvents were of reagent grade and were used without further purification unless stated otherwise. Reactions were monitored by thin-layer chromatography (TLC) carried out on 0.25 mm Merck silica gel aluminum plates, using UV light as visualizing agent. Silica gel was used for column chromatography. <sup>1</sup>H and <sup>13</sup>C NMR spectra were recorded on a Varian Unity 300 MHz spectrometer; <sup>1</sup>H and <sup>13</sup>C chemical shifts were referenced with the residual solvent resonances relative to tetramethylsilane. IR spectra were recorded as KBr pellets or in CsI cells on a Perkin-Elmer 577 spectrometer. The starting materials (NEt<sub>4</sub>)<sub>2</sub>[ReBr<sub>3</sub>(CO)<sub>3</sub>] (**1**), [<sup>99m</sup>Tc(OH)<sub>2</sub>(CO)<sub>3</sub>]<sup>+</sup> (**1a**), the ligands **L**<sup>1</sup>–**L**<sup>3</sup> and **L**<sup>5</sup>, and

the complexes [Re(CO)<sub>3</sub>(k<sup>3</sup>-L)]Br (L = **L**<sup>1</sup> (**2**), **L**<sup>2</sup> (**3**), **L**<sup>3</sup> (**4**), **L**<sup>5</sup> (**6**)) were prepared according to published methods (**9**, **10**, **20**, **21**, **29**–**31**).

Peptide synthesis was performed on a Perkin-Elmer-Applied Biosystem model 432 automated peptide synthesizer employing traditional Fmoc chemistry. The preselected synthetic sequence was designed to produce the **L**<sup>6</sup>-(X)-BBN conjugate with the following general structure **L**<sup>6</sup>-X-Q-W-A-V-G-H-L-M-NH<sub>2</sub>, where the spacer group, X = GlycylGlycylGlycine. The crude peptide was purified by HPLC, and the solvents were removed on a SpeedVac concentrator. Typical yields of the crude peptide were 80–85%. ES-MS was used to determine the molecular constitution of the **L**<sup>6</sup>-(X)-BBN[7-14]NH<sub>2</sub> conjugate. Na[<sup>99m</sup>TcO<sub>4</sub>] was eluted from a <sup>99</sup>Mo/<sup>99m</sup>Tc generator using 0.9% saline. HPLC analysis of the Re and <sup>99m</sup>Tc complexes was performed on a Shimadzu C-R4A chromatography system equipped with a Berthold-LB 505  $\gamma$ -detector and with a tunable absorption UV detector. Separations were achieved on Nucleosil 250-4 100-10 C18 columns or on 250-4 100-5 C18 columns, using flows of 1 or 0.5 mL/min, respectively; UV detection, 254 nm; eluents, A-TFA 0.1%, B-MeOH; method, *t* = 0–3 min, 0% MeOH; 3–3.1 min, 0–25% MeOH; 3.1–9 min, 25% MeOH; 9–9.1 min, 25–34% MeOH; 9.1–20 min, 34–100% MeOH; 20–22 min, 100% MeOH; 22–22.1 min, 100–0% MeOH; 22.1–30 min, 0% MeOH. HPLC evaluation of the nonmetalated and metalated BBN-conjugate was performed using experimental conditions similar to those referenced above. However, the eluenting solvents were water with 0.1% TFA (A) and CH<sub>3</sub>CN 0.1% TFA (B), and the wavelength of detection was 280 nm.

**Synthesis of pz(CH<sub>2</sub>)<sub>2</sub>NH(CH<sub>2</sub>)<sub>2</sub>NH<sub>2</sub> (**L**<sup>4</sup>).** A solution of 1-(2-bromoethyl)pyrazole (**32**) (2.1 g, 12 mmol) in THF (10 mL) was added dropwise to a solution of ethylenediamine (14.4 g, 0.24 mol) in H<sub>2</sub>O (20 mL). After refluxing for 4 h, the THF was removed under vacuum, and the residual water phase was washed with CH<sub>2</sub>Cl<sub>2</sub>. The aqueous phase was vacuum-dried with mild heating to eliminate some remaining ethylenediamine. Compound **L**<sup>4</sup> was obtained as a yellow oil, which darkened to brown with heating. Yield: 924 mg, 50%. <sup>1</sup>H NMR (D<sub>2</sub>O): 7.53 (d, H(3)pz, 1H); 7.45 (d, H(5)pz, 1H); 6.23 (t, H(4)pz, 1H); 4.14 (t, CH<sub>2</sub>, 2H); 2.91 (t, CH<sub>2</sub>, 2H); 2.77 (t, CH<sub>2</sub>, 2H); 2.62 (t, CH<sub>2</sub>, 2H). <sup>13</sup>C NMR (CD<sub>3</sub>OD): 140.3 (C(3,5)pz); 131.9 (C(3,5)pz); 106.5 (C(4)pz); 52.48 (CH<sub>2</sub>); 49.93 (CH<sub>2</sub>); 41.60 (CH<sub>2</sub>); 40.32 (CH<sub>2</sub>). IR( $\nu$ /cm<sup>-1</sup>) (CsI): 1651, 1094, 1034, 763.

**Synthesis of 3,5Me<sub>2</sub>-pz(CH<sub>2</sub>)<sub>2</sub>N((CH<sub>2</sub>)<sub>3</sub>COOH)-(CH<sub>2</sub>)<sub>2</sub>NH<sub>2</sub> (**L**<sup>6</sup>) and pz(CH<sub>2</sub>)<sub>2</sub>N((CH<sub>2</sub>)<sub>3</sub>COOH)(CH<sub>2</sub>)<sub>2</sub>-NH<sub>2</sub> (**L**<sup>7</sup>).** **L**<sup>6</sup>: An equimolar amount of BOC-ON in THF

was added dropwise to a solution of  $L^2$  (4.0 g, 22.5 mmol) in THF (70 mL) at 0 °C, and the reaction mixture was left at this temperature for 3 h. A saturated aqueous solution of  $Na_2CO_3$  and  $CH_2Cl_2$  was added at room temperature, and the organic phase was separated, dried over anhydrous  $MgSO_4$ , and vacuum-dried. The yellow oil that was obtained,  $L^2$ -Boc (5.7 g, 20 mmol), was dissolved in  $CH_3CN$  (60 mL), and an excess of  $K_2CO_3$ , KI, and ethyl 4-bromobutyrate was added. After 11 days at room temperature, the solution was filtered, vacuum-dried, and the residue was purified by column chromatography (ethyl acetate (50–100%)/hexane). The BOC protected derivative (4 g, 10.2 mmol) was dissolved in THF, and an excess of NaOH added and refluxed overnight, for saponification of the ethyl ester. The solution was neutralized with HCl (1 N), the solvents were removed, and the residue was extracted with  $CH_2Cl_2$ . The crude product was purified by column chromatography (MeOH (5–100%)/ $CHCl_3$ ), and the pale yellow oil (2.2 g, 86%) was treated with an excess of TFA in  $CH_2Cl_2$  to remove the BOC protecting group. Evaporation of the solvent, addition of  $H_2O$ , neutralization with 1 N HCl, and extraction with a small amount of MeOH led to a suspension, which, after being filtered off, was vacuum-dried yielding a pale yellow oil, which crystallizes upon standing. Yield: 2.07 g, 36%.  $^1H$  NMR ( $CD_3OD$ ): 5.83 (s, H(4)pz, 1H); 4.07 (t,  $CH_2$ , 2H); 2.98 (t,  $CH_2$ , 2H); 2.77 (t,  $CH_2$ , 2H); 2.70 (t,  $CH_2$ , 2H); 2.48 (t,  $CH_2$ , 2H); 2.26 (s,  $CH_3$ , 3H); 2.16 (s,  $CH_3$ , 3H); 2.00 (t,  $CH_2$ , 2H); 1.62 (q,  $CH_2$ , 2H).  $^{13}C$  NMR ( $CD_3OD$ ): 183.3 (COOH); 148.4 (C(3)pz); 141.0 (C(5)pz); 106.2 (C(4)pz); 54.1 ( $CH_2$ ); 54.0 ( $CH_2$ ); 52.0 ( $CH_2$ ); 47.2 ( $CH_2$ ); 38.5 ( $CH_2$ ); 36.0 ( $CH_2$ ); 24.8 ( $CH_2$ ); 13.1 ( $CH_3$ ); 10.9 ( $CH_3$ ). IR ( $\nu/cm^{-1}$ ) (KBr):  $\nu(C=O)$  1694, 1559, 1442, 1210, 845, 804, 725.

$L^7$ : This compound was prepared as described for  $L^6$  (vide infra). Starting with 1.1 g (7 mmol) of  $L^4$  in DMF, a brownish oil formulated as  $L^7$  was obtained. Yield: 403 mg, 24%.  $^1H$  NMR ( $D_2O$ ): 7.58 (s, H(3)pz, 1H); 7.48 (s, H(5)pz, 1H); 6.25 (t, H(4)pz, 1H); 4.49 (t,  $CH_2$ , 2H); 3.64 (t,  $CH_2$ , 2H); 3.42 (t,  $CH_2$ , 2H); 3.25 (t,  $CH_2$ , 2H); 3.12 (t,  $CH_2$ , 2H); 2.30 (t,  $CH_2$ , 2H); 1.79 (q,  $CH_2$ , 2H).  $^{13}C$  NMR ( $CD_3OD$ ): 180.0 (COOH); 140.1 (C(3)pz); 131.8 (C(5)pz); 106.7 (C(4)pz); 54.9 ( $CH_2$ ); 54.1 ( $CH_2$ ); 52.0 ( $CH_2$ ); 50.7 ( $CH_2$ ); 38.6 ( $CH_2$ ); 33.9 ( $CH_2$ ); 23.9 ( $CH_2$ ). IR (CsI) ( $\nu/cm^{-1}$ ):  $\nu(C=O)$  1685, 1442, 1209, 1138, 845, 803, 763.

**Synthesis of 3,5Me<sub>2</sub>-pz(CH<sub>2</sub>)<sub>2</sub>N(CH<sub>2</sub>)<sub>3</sub>(glylygly-OEt)(CH<sub>2</sub>)<sub>2</sub>NH<sub>2</sub> ( $L^8$ ) and pz(CH<sub>2</sub>)<sub>2</sub>N(CH<sub>2</sub>)<sub>3</sub>(glylygly-OEt)(CH<sub>2</sub>)<sub>2</sub>NH<sub>2</sub> ( $L^9$ ).** Compounds  $L^6$ -BOC or  $L^7$ -BOC,  $NEt_3$  and HBTU, in the molar ratio 1:3:1, were dissolved in  $CH_3CN$ . To the resulting solutions were added equimolar amounts of glylyglycine ethyl ester (196 mg, 1 mmol). After reaction at room temperature, the solvent was evaporated and the residues were purified by column chromatography (MeOH (5–20%)/ $CHCl_3$ ) or by dissolving the crude product in  $CHCl_3$  and washing three times with  $H_2O$ . The BOC protecting group was removed with TFA. After 1 h at room temperature, the solvent was evaporated, and the residue was dissolved in  $H_2O$  and neutralized with NaOH(1N). Compound  $L^8$  was obtained as a pale yellow oil upon evaporation of  $H_2O$  and purification by column chromatography (MeOH (20–50%)/ $CHCl_3$ ). Compound  $L^9$  was obtained as a yellow oil upon removal of  $H_2O$  and extraction with MeOH.

$L^8$ : Yield: 179 mg, 45%.  $^1H$  NMR ( $D_2O$ ): 5.80 (s, H(4)pz, 1H); 4.04 (q,  $CH_2CH_3$ , 2H); 3.91 (t,  $CH_2$ , 2H); 3.85 (s,  $NHCH_2$ , 2H); 3.80 (s,  $NHCH_2$ , 2H); 2.81 (t,  $CH_2$ , 2H); 2.71 (t,  $CH_2$ , 2H); 2.59 (t,  $CH_2$ , 2H); 2.38 (t,  $CH_2$ , 2H); 2.10 (m,  $CH_2 + CH_3$ , 5H); 2.00 (s,  $CH_3$ , 3H); 1.53 (q,  $CH_2$ , 2H); 1.09 (t,  $CH_3$ , 3H).  $^{13}C$  NMR ( $CD_3OD$ ): 176.5 (CO);

172.3 (CO); 171.4 (CO); 148.5 (C(3)pz); 141.2 (C(5)pz); 106.3 (C(4)pz); 62.4 ( $CH_2$ ); 54.0 ( $CH_2$ ); 53.9 ( $CH_2$ ); 52.0 ( $CH_2$ ); 47.1 ( $CH_2$ ); 43.2 ( $CH_2$ ); 41.9 ( $CH_2$ ); 38.6 ( $CH_2$ ); 33.6 ( $CH_2$ ); 23.8 ( $CH_2$ ); 14.4 ( $CH_3$ ); 13.2 ( $CH_3$ ); 10.9 ( $CH_3$ ). IR (CsI) ( $\nu/cm^{-1}$ ):  $\nu(C=O)$  1680, 1552, 1440, 1207, 1138, 1031, 842, 803, 724.

$L^9$ : Yield: 121 mg, 33%.  $^1H$  NMR ( $D_2O$ ): 7.56 (d, H(3)pz, 1H); 7.46 (d, H(5)pz, 1H); 6.22 (t, H(4)pz, 1H); 4.46 (t,  $CH_2$ , 2H); 3.95 (m,  $CH_2CH_3$ , 2H); 3.72 (m, 2 $CH_2$ , 4H); 3.59 (t,  $CH_2$ , 2H); 3.38 (t,  $CH_2$ , 2H); 3.22 (t,  $CH_2$ , 2H); 3.09 (t,  $CH_2$ , 2H); 2.25 (t,  $CH_2$ , 2H); 1.76 (m,  $CH_2$ , 2H); 1.02 (t,  $CH_3$ , 3H).  $^{13}C$  NMR ( $CD_3OD$ ): 176.2 (CO); 173.0 (CO); 172.0 (CO); 141.2 (C(3)pz); 132.3 (C(5)pz); 107.3 (C(4)pz); 62.4 ( $CH_2$ ); 55.0 ( $CH_2$ ); 54.6 ( $CH_2$ ); 51.5 ( $CH_2$ ); 47.8 ( $CH_2$ ); 43.4 ( $CH_2$ ); 41.7 ( $CH_2$ ); 36.4 ( $CH_2$ ); 33.5 ( $CH_2$ ); 21.4 ( $CH_2$ ); 14.4 ( $CH_3$ ). IR (CsI) ( $\nu/cm^{-1}$ ):  $\nu(C=O)$  1677, 1426, 1202, 1135, 837, 800, 722.

**Synthesis of the Re(I) Complexes (5 and 7–10).** *General Method.* ( $NEt_3$ )<sub>2</sub>[ReBr<sub>3</sub>(CO)<sub>3</sub>] (1) (100 mg, 0.130 mmol) was reacted with equimolar amounts of the compounds  $L^4$  and  $L^6$ – $L^9$  in refluxing  $H_2O$  for 2 h or overnight. The complexes precipitate as white solids from the aqueous solutions upon concentration and cooling. Compounds 5 and 7–10 were obtained in yields between 75% and 85%. With the exception of 10, the characterization of all complexes was achieved by IR,  $^1H$ , and  $^{13}C$  NMR spectroscopies and ES/MS. The identification of 10 involved only IR and ES/MS.

**[Re(CO)<sub>3</sub>( $\kappa^3$ -pz(CH<sub>2</sub>)<sub>2</sub>NH(CH<sub>2</sub>)<sub>2</sub>NH<sub>2</sub>)]Br (5).**  $^1H$  NMR ( $D_2O$ ): 7.82 (d, H(3)pz, 1H); 7.76 (d, H(5)pz, 1H); 6.54 (s, br, NH, 1H); 6.39 (t, H(4)pz, 1H); 4.86 (s, br, NH<sub>2</sub>, 1H); 4.43 (m,  $CH_2$ , 1H); 4.16 (m,  $CH_2$ , 1H); 3.94 (s, br, NH<sub>2</sub>, 1H); 3.50 (m,  $CH_2$ , 1H); 2.87 (m,  $CH_2$ , 1H); 2.71 (m,  $CH_2$ , 2H); 2.48 (m,  $CH_2$ , 1H); 2.08 (m,  $CH_2$ , 1H).  $^{13}C$ -RMN ( $CD_3OD$ ): 198.2 (ReCO); 194.8 (ReCO); 194.7 (ReCO); 146.6 (C(3)pz); 135.6 (C(5)pz); 108.7 (C(4)pz); 56.0 ( $CH_2$ ); 49.0 (2 $CH_2$ ); 41.8 ( $CH_2$ ). IR ( $\nu/cm^{-1}$ ):  $\nu(C=O)$ , 2020, 1920, 1890, 1599, 1461, 1283, 1197, 1078, 941, 758.

**[Re(CO)<sub>3</sub>( $\kappa^3$ -3,5Me<sub>2</sub>-pz(CH<sub>2</sub>)<sub>2</sub>N((CH<sub>2</sub>)<sub>3</sub>COOH)-(CH<sub>2</sub>)<sub>2</sub>NH<sub>2</sub>)]Br (7).**  $^1H$  NMR ( $CD_3OD$ ):  $\delta$  6.20 (s, H(4)pz, 1H); 5.53 (s, br, NH<sub>2</sub>, 1H); 4.58–4.52 (m,  $CH_2$ , 1H); 4.26–4.17 (m,  $CH_2$ , 1H); 4.10 (s, br, NH<sub>2</sub>, 1H); 3.69 (m,  $CH_2$ , 1H); 3.53 (m,  $CH_2$ , 2H); 3.06 (m,  $CH_2$ , 1H); 2.90 (m,  $CH_2$ , 2H); 2.72 (m,  $CH_2$ , 1H); 2.55 (m,  $CH_2$ , 1H); 2.45 (s,  $CH_3$ , 3H); 2.38 (s,  $CH_3$ , 3H); 2.18 (m,  $CH_2$ , 2H); 2.04 (m,  $CH_2$ , 2H).  $^{13}C$ -RMN ( $CD_3OD$ ): 195.4 (3CO); 176.2 (COOH); 155.1 (C-pz); 145.3 (C-pz); 109.2 (C-pz); 67.1 ( $CH_2$ ); 62.4 ( $CH_2$ ); 53.7 ( $CH_2$ ); 43.6 ( $CH_2$ ); 31.5 ( $CH_2$ ); 30.9 ( $CH_2$ ); 20.5 ( $CH_2$ ); 16.1 ( $CH_3$ ); 11.6 ( $CH_3$ ). IR ( $\nu/cm^{-1}$ ):  $\nu(C=O)$ , 2031, 1974, 1901;  $\nu(C=O)$  1686, 1432, 1205, 1143, 848, 800, 728, 588. ES/MS (+) (referenced to the species with  $^{187}Re$ ; relative abundance in parentheses):  $m/z$  539 (100%) [ $M$ ]<sup>+</sup>.

**[Re(CO)<sub>3</sub>( $\kappa^3$ -pz(CH<sub>2</sub>)<sub>2</sub>N((CH<sub>2</sub>)<sub>3</sub>COOH)(CH<sub>2</sub>)<sub>2</sub>NH<sub>2</sub>)]Br (8).**  $^1H$  NMR ( $D_2O$ ):  $\delta$  7.86 (t, H(3)pz, 1H); 7.81 (t, H(5)pz, 1H); 6.44 (s, H(4)pz, 1H); 5.07 (s br, NH<sub>2</sub>, 1H); 4.52 (m,  $CH_2$ , 1H); 4.37 (m,  $CH_2$ , 1H); 4.10 (s br, NH<sub>2</sub>, 1H); 3.58 (m,  $CH_2$ , 1H); 3.40 (m,  $CH_2$ , 2H); 2.89 (m,  $CH_2$ , 1H); 2.70 (m,  $CH_2$ , 1H); 2.40 (m,  $CH_2$ , 2H); 2.33 (m,  $CH_2$ , 1H); 2.13 (m,  $CH_2$ , 2H); 1.97 (m,  $CH_2$ , 2H).  $^{13}C$ -RMN ( $CD_3OD$ ): 198.2–193.8 (3CO); 185.3 (COOH); 146.6 (C-pz); 135.8 (C-pz); 108.9 (C-pz); 67.9 ( $CH_2$ ); 63.0 ( $CH_2$ ); 54.5 ( $CH_2$ ); 52.0 ( $CH_2$ ); 43.3 ( $CH_2$ ); 31.6 ( $CH_2$ ); 20.8 ( $CH_2$ ). IR (KBr) ( $\nu/cm^{-1}$ ):  $\nu(C=O)$ , 2023, 1901;  $\nu(C=O)$ , 1680, 1202, 1146, 1076, 852, 793, 762, 729. ES/MS (+) (referenced to the species with  $^{187}Re$ ; relative abundance in parentheses):  $m/z$  511 (100%) [ $M$ ]<sup>+</sup>.

**[Re(CO)<sub>3</sub>( $\kappa^3$ -3,5Me<sub>2</sub>-pz(CH<sub>2</sub>)<sub>2</sub>N(glylygly)(CH<sub>2</sub>)<sub>2</sub>NH<sub>2</sub>)]Br (9).**  $^1H$  NMR ( $D_2O$ ):  $\delta$  6.04 (s, H(4)pz, 1H); 5.05 (s, br, NH<sub>2</sub>, 1H); 4.30 (m,  $CH_2$ , 1H); 4.05 (m,  $CH_2$ , 1H); 3.88

(s,  $\text{NHCH}_2\text{CO}$ , 2H); 3.84 (s,  $\text{NHCH}_2\text{CO}$ , 2H); 3.65 (s, br,  $\text{NH}_2$ , 1H); 3.53 (m,  $\text{CH}_2$ , 1H); 3.30 (m,  $\text{CH}_2$ , 2H); 2.86 (m,  $\text{CH}_2$ , 1H); 2.74 (m,  $\text{CH}_2$ , 2H); 2.57 (m,  $\text{CH}_2$ , 1H); 2.40 (m,  $\text{CH}_2$ , 1H); 2.73 (s,  $\text{CH}_3$ , 3H); 2.16 (s,  $\text{CH}_3$ , 3H); 2.10 (m,  $\text{CH}_2$ , 2H); 1.95 (m,  $\text{CH}_2$ , 2H).

$^{13}\text{C}$  NMR ( $\text{CD}_3\text{OD}$ ): 195.2 (ReCO); 194.8 (ReCO); 193.8 (ReCO); 175.2 (CO); 172.2 (CO); 171.3 (CO); 155.0 (C(3)pz); 145.3 (C(5)pz); 109.2 (C(4)pz); 67.1 ( $\text{CH}_2$ ); 62.4 ( $\text{CH}_2$ ); 53.8 ( $\text{CH}_2$ ); 49.0 ( $\text{CH}_2$ ); 43.7 ( $\text{CH}_2$ ); 42.0 ( $\text{CH}_2$ ); 33.3 ( $\text{CH}_2$ ); 21.1 ( $\text{CH}_2$ ); 16.2 ( $\text{CH}_3$ ); 11.7 ( $\text{CH}_3$ ). IR (KBr) ( $\nu/\text{cm}^{-1}$ ):  $\nu(\text{C}=\text{O})$ , 2015, 1876;  $\nu(\text{C}=\text{O})$  1697, 1458, 1412, 1190, 1139, 850, 791, 729. ES/MS (referenced to the species with  $^{187}\text{Re}$ ; relative abundance in parentheses):  $m/z$  653 (100%)  $[\text{M}]^+$ .

**[Re(CO) $_3$ ( $\kappa^3$ -pz( $\text{CH}_2$ ) $_2$ N( $\text{CH}_2$ ) $_3$ (glygly)( $\text{CH}_2$ ) $_2$ NH $_2$ )]-Br (10).** IR (CsI) ( $\nu/\text{cm}^{-1}$ ):  $\nu(\text{C}=\text{O})$  2014, 1891;  $\nu(\text{C}=\text{O})$  1689, 1460, 1397, 1204, 1136, 1003, 837, 800. ES/MS (referenced to the species with  $^{187}\text{Re}$ ; relative abundance in parentheses):  $m/z$  625 (100%)  $[\text{M}]^+$ .

**Synthesis of the  $^{99\text{m}}\text{Tc}(\text{I})$  Complexes (2a–6a, 9a–11a).** *General Method.* In a nitrogen-purged glass vial, 100  $\mu\text{L}$  of a  $10^{-3}$  or  $10^{-4}$  M solution of the compounds  $\text{L}^1$ – $\text{L}^6$ ,  $\text{L}^9$ ,  $\text{L}^{10}$ , and  $[\text{L}^6\text{-(GGG)-Bombesin(7-14)NH}_2]$  were added to 900  $\mu\text{L}$  of a solution of *fac*- $^{99\text{m}}\text{Tc}(\text{OH})_3(\text{CO})_3]^+$  (1–2 mCi) in PBS. The reaction mixture was incubated at 100  $^\circ\text{C}$  for 30–60 min and then analyzed by HPLC.

**Cysteine and Histidine Challenge.** Aliquots of 100  $\mu\text{L}$  of the  $^{99\text{m}}\text{Tc}$  complexes were added to 900  $\mu\text{L}$  of  $10^{-3}$  M cysteine or histidine solutions in PBS (pH 7.4) (final ligand concentration  $10^{-5}$  M). The solutions were incubated at 37  $^\circ\text{C}$ , and aliquots were removed at 1, 2, 4, and 6 h, at which time HPLC analysis was run.

**Lipophilicity.** The lipophilicity of the compounds was evaluated by determination of the partition coefficient ( $P$ ) in physiological conditions (*n*-octanol/0.1 M PBS, pH 7.4).

**Biodistribution Analysis of Complexes 2a–6a and 9a,10a in Normal, CD-1, Mouse Models.** Biodistribution studies were performed using groups of five female CD-1 mice (randomly bred, Charles River) weighing approximately 20–25 g each. Prior to administration, complexes were diluted with PBS pH = 7.4. Animals were intravenously injected with 100  $\mu\text{L}$  (2.5–12.5 MBq) of each preparation via the tail vein and were maintained on normal diet ad libitum. At 5 min, 30 min, 1 h, and 4 h, mice were sacrificed by cervical dislocation. The administered dose and the radioactivity in the sacrificed animals were measured in a dose calibrator (Aloka, Curiometer IGC-3, Tokyo, Japan). The difference between the radioactivity in the injected and sacrificed animal was assumed to be due to excretion, mainly urinary excretion. Blood samples were taken by cardiac puncture at sacrifice. Tissue samples of the main organs were then removed, weighed, and counted in a gamma counter (Berthold, LB2111, Germany). Accumulation of radioactivity in the tissues was calculated and expressed as percentage of the injected dose per total organ (% ID/total organ) and/or per gram tissue (% ID/g organ). For blood, bone, and muscle, total activity was calculated assuming that these organs constitute 6%, 10%, and 40% of the total weight, respectively. Urine was also collected at the time of sacrifice.

The *in vivo* stability of the complexes was assessed by urine and murine serum HPLC analysis, using the above referenced experimental conditions. Urine: the urine was collected at sacrifice time and filtered through a Millex GV filter (0.22  $\mu\text{m}$ ) before RP-HPLC analysis. Serum: Blood collected from mice was immediately centrifuged for 15 min at 3000 rpm at 4  $^\circ\text{C}$ , and the serum was separated. Aliquots of 100  $\mu\text{L}$  of serum were treated with

200  $\mu\text{L}$  of ethanol to precipitate the proteins. Samples were centrifuged at 4000 rpm for 15 min, at 4  $^\circ\text{C}$ . Supernatant was collected and passed through a Millex GV filter (0.22  $\mu\text{m}$ ) prior to RP-HPLC analysis. Liver homogenate: After injection, animals were kept for 1 h on normal diet ad libitum, and, immediately after sacrifice, the liver was excised and rapidly rinsed and placed in chilled 50 mM TRIS/0.2 M sucrose buffer, pH = 7.4, wherein it was homogenized. Aliquots (in duplicate) of the liver homogenate were treated with ethanol in a 2:1 EtOH/aliquot v/v ratio. The samples were then centrifuged at 25 000 rpm for 15 min at 4  $^\circ\text{C}$ , filtered through Millex GV (0.22  $\mu\text{m}$ ), and analyzed by HPLC, following the experimental conditions referred above.

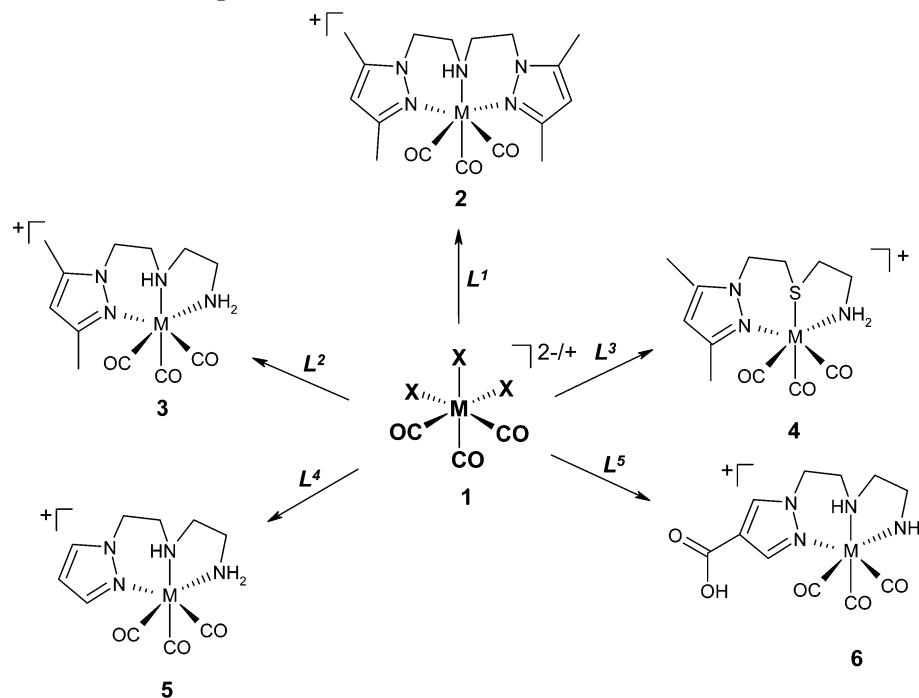
**In Vitro Cell Binding Affinity Studies of  $^{99\text{m}}\text{Tc-L}^6\text{-(GGG)-Bombesin(7-14)NH}_2$  (11a).** *In Vitro Receptor Binding.* The  $\text{IC}_{50}$  (inhibitory concentration 50%) value of  $[\text{L}^6\text{-(GGG)-Bombesin(7-14)NH}_2]$  was determined by a competitive displacement cell binding assay using  $^{125}\text{I-Tyr}^4\text{-Bombesin}$  as the radiolabel. Briefly,  $\sim 3 \times 10^6$  cells (Suspended in D-MEM/F-12K media containing 0.01 M MEM and 2% BSA, pH = 5.5) were incubated at 37  $^\circ\text{C}$  for 1 h in the presence of 20 000 cpm  $^{125}\text{I-Tyr}^4\text{-Bombesin}$  and increasing concentrations of nonradiolabeled conjugate. Upon completion of the incubation, the reaction medium was aspirated and the cells were washed four times with media. Cell-associated radioactivity was determined by counting in a Packard Riastar gamma counting system.

**Internalization and Efflux Evaluation.** *In vitro* internalization analysis of  $^{99\text{m}}\text{Tc}(\text{CO})_3\text{-L}^6\text{-(GGG)-Bombesin(7-14)NH}_2$  was carried out by incubation of  $\sim 3 \times 10^6$  cells (in D-MEM/F-12K media containing 0.01 M MEM and 2% BSA, pH = 5.5) in the presence of 20 000 cpm labeled conjugate at 37  $^\circ\text{C}$  for selected timepoints of 15, 30, 45, 60, and 90 min. Upon completion of the incubation, the reaction medium was aspirated and the cells were washed four times with media. Surface-bound radioactivity was removed by washing the cells with 0.2 N acetic acid/0.5 M NaCl (pH = 2.5). The percent of internalized, cell-associated, radioactivity as a function of time was determined by counting in a Packard Riastar gamma counting system. Efflux evaluation was performed after a 45 min internalization period. The cellular medium was washed (3 $\times$ ) with buffer (room temperature) and resuspended for further incubation. Selected sampling at 0, 15, 30, 45, 60, and 90 min postinternalization was performed by an initial cold buffer wash of the cells, followed by washing with acetic acid/saline (pH = 2.5 at 4  $^\circ\text{C}$ ).

**Biodistribution Analysis of  $^{99\text{m}}\text{Tc-L}^6\text{-(GGG)-Bombesin(7-14)NH}_2$  in Normal, CF-1, Mouse Models.** The biodistribution study of  $^{99\text{m}}\text{Tc-L}^6\text{-(GGG)-Bombesin(7-14)NH}_2$  was determined in normal, CF-1 mice at the University of Missouri–Columbia. The mice were injected with 5  $\mu\text{Ci}$  (185 kBq) of the complex in 100  $\mu\text{L}$  of isotonic saline via the tail vein. The mice were euthanized, and the tissues and organs were excised from the animals following at 1, 4, and 24 h postinjection (p.i.) Subsequently, the tissues and organs were weighed and counted in a NaI well counter and the percent injected dose (% ID) and % ID/g of each organ or tissue calculated. The % ID in whole blood was estimated assuming a whole-blood volume of 6.5% the total body weight.

## RESULTS AND DISCUSSION

**Pyrazolyl-Based  $^{99\text{m}}\text{Tc}$ -Building Blocks.** Following our previous work (20–22) and profiting from the ver-

**Scheme 1. Synthesis of Metal Complexes (M = Re, X = Br (2–6) and M = <sup>99m</sup>Tc, X = H<sub>2</sub>O (2a–6a))****Table 1. Experimental Conditions for the Synthesis of Complexes 2a–6a and Characteristics of the Complexes**

complex	yield [%]	<i>c</i> [M]	<i>t</i> [min]	<i>T</i> (°C)	RT (min) <sup>a</sup>	log <i>P</i> <sub>o/w</sub> ± <i>s</i>
<b>2a</b> ( <i>L</i> <sup>1</sup> )	>90	10 <sup>−4</sup>	30	100	16.7 (16.2) <sup>b</sup>	0.87 ± 0.03
<b>3a</b> ( <i>L</i> <sup>2</sup> )	>99	10 <sup>−5</sup>	30	100	24.2 (23.4) <sup>c</sup>	−0.24 ± 0.03
<b>4a</b> ( <i>L</i> <sup>3</sup> )	>95	10 <sup>−5</sup>	30	100	19.8 (19.4) <sup>b</sup>	−0.07 ± 0.01
<b>5a</b> ( <i>L</i> <sup>4</sup> )	>95	10 <sup>−5</sup>	30	100	16.9 (16.5) <sup>c</sup>	−0.93 ± 0.01
<b>6a</b> ( <i>L</i> <sup>5</sup> ) <sup>20b</sup>	>95	10 <sup>−4</sup>	30	100	18.8 (18.2) <sup>b</sup>	−2.35 ± 0.01

<sup>a</sup> The values in parentheses are for the Re complexes. <sup>b</sup> Nucleosil 250-4 100-10 C18 columns, flow of 1 mL/min. <sup>c</sup> Nucleosil 250-4 100-5 C18 columns, flow of 0.5 mL/min.

satility of the symmetric (*L*<sup>1</sup>) and asymmetric (*L*<sup>2</sup>–*L*<sup>5</sup>) pyrazolyl-containing ligands, we evaluated the behavior of these compounds toward the *fac*-[<sup>99m</sup>Tc(CO)<sub>3</sub>]<sup>+</sup> moiety. We intended to assess the influence of using symmetric and asymmetric ligands, having different pyrazolyl substituents (−H, −CH<sub>3</sub>, −COOH) and/or donor atom sets, on the physicochemical and biological properties of the corresponding <sup>99m</sup>Tc complexes.

The ligands *L*<sup>1</sup>–*L*<sup>3</sup> and *L*<sup>5</sup>, as well as the corresponding tricarbonyl rhenium complexes **2**–**4** and **6**, were already available, and their synthesis and characterization has been previously reported by our group (20, 21). In contrast, the lighter member of this family of ligands, compound *L*<sup>4</sup>, which was not described previously, has been obtained by refluxing 1-(2-bromoethyl)pyrazole with an excess of ethylenediamine in a mixture of THF/H<sub>2</sub>O, and its characterization was done by <sup>1</sup>H and <sup>13</sup>C NMR spectroscopy. Reaction of the mixed halide-carbonyl (NEt<sub>4</sub>)<sub>2</sub>[ReBr<sub>3</sub>(CO)<sub>3</sub>] (**1**) with *L*<sup>4</sup> in water yielded [Re(CO)<sub>3</sub>(k<sup>3</sup>-*L*<sup>4</sup>)]Br (**5**) (Scheme 1). The IR, <sup>1</sup>H, and <sup>13</sup>C NMR spectroscopic data obtained for **5** are compatible with the tridentate coordination mode of *L*<sup>4</sup> and compare well with the results previously found for the complexes [Re(CO)<sub>3</sub>(k<sup>3</sup>-*L*)]Br (*L* = *L*<sup>2</sup> (**3**), *L*<sup>3</sup> (**4**)), which were characterized both in the solid state and in solution (Scheme 1) (20, 21).

The <sup>99m</sup>Tc-building blocks [<sup>99m</sup>Tc(CO)<sub>3</sub>(k<sup>3</sup>-*L*)]<sup>+</sup> (*L* = *L*<sup>1</sup>–*L*<sup>5</sup> (**2a**–**6a**)) have been obtained by reacting [<sup>99m</sup>Tc(CO)<sub>3</sub>(OH<sub>2</sub>)<sub>3</sub>]<sup>+</sup> (**1a**) with aliquots of standard solutions of the corresponding pyrazolyl ligands, in a total volume of 1 mL (Scheme 1). The compounds formed were identified by comparing their HPLC chromatograms with the

HPLC profiles of the analogues Re complexes, fully characterized either in the solid state and/or in solution (20, 21).

The labeling conditions, the labeling yields, the log *P*<sub>o/w</sub>, and the retention times for the <sup>99m</sup>Tc complexes are shown in Table 1. Under optimized labeling conditions, all complexes were obtained in almost quantitative yield (≥90%), with final concentration of the ligands (*L*) spanning from 10<sup>−4</sup> to 10<sup>−5</sup> M.

Complexes **2a**–**6a** were challenged in 1 mM cysteine and histidine solutions at 37 °C. The samples were analyzed by HPLC at 1, 2, 4, and 6 h, and the results obtained have confirmed a high stability for the complexes. Even for the less stable complex **2a**, almost no degradation or trans-chelation was observed, as can be confirmed by the data shown in Figure 1.

The biological distribution of the tricarbonyl complexes **2a**–**6a** was assessed in CD-1 mice at 5 min, 1 h, and 4 h after administration. Tissue distribution data of these complexes were expressed as the percentage of injected dose per gram of organ, and the uptake and clearance from most relevant organs can be overviewed in the histogram shown in Figure 2. Just for comparison, we also present in Table 2 the biodistribution of these complexes 4 h after administration. Total excretion of radioactivity over time is graphically represented in Figure 3.

The data show that all of the <sup>99m</sup>Tc-tricarbonyl complexes under study were rapidly cleared from blood and other main organs, primarily the renal-urinary pathway with a small portion retained in the hepatobiliary tract. The main differences in the biodistribution of the differ-

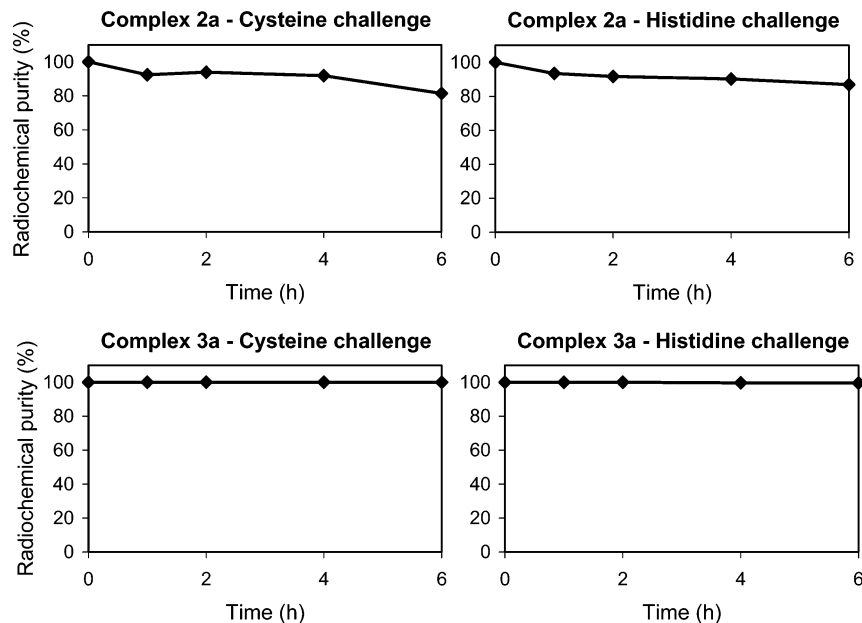


Figure 1. Stability of 2a and 3a in 1 mM cysteine and histidine solutions, at 37 °C.

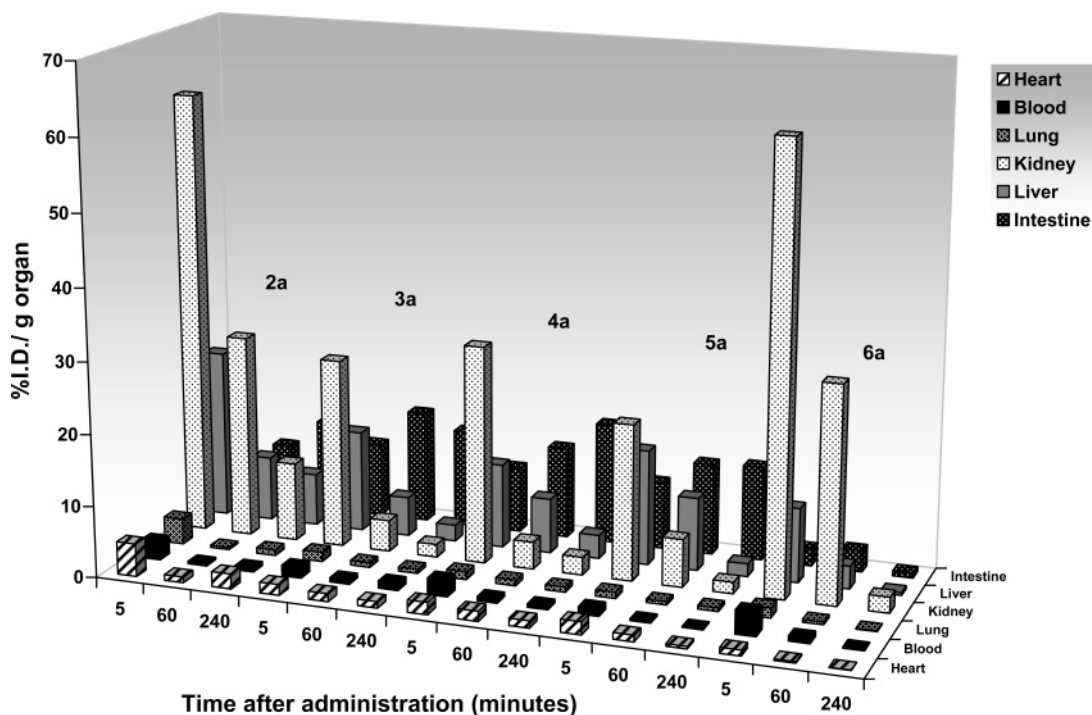


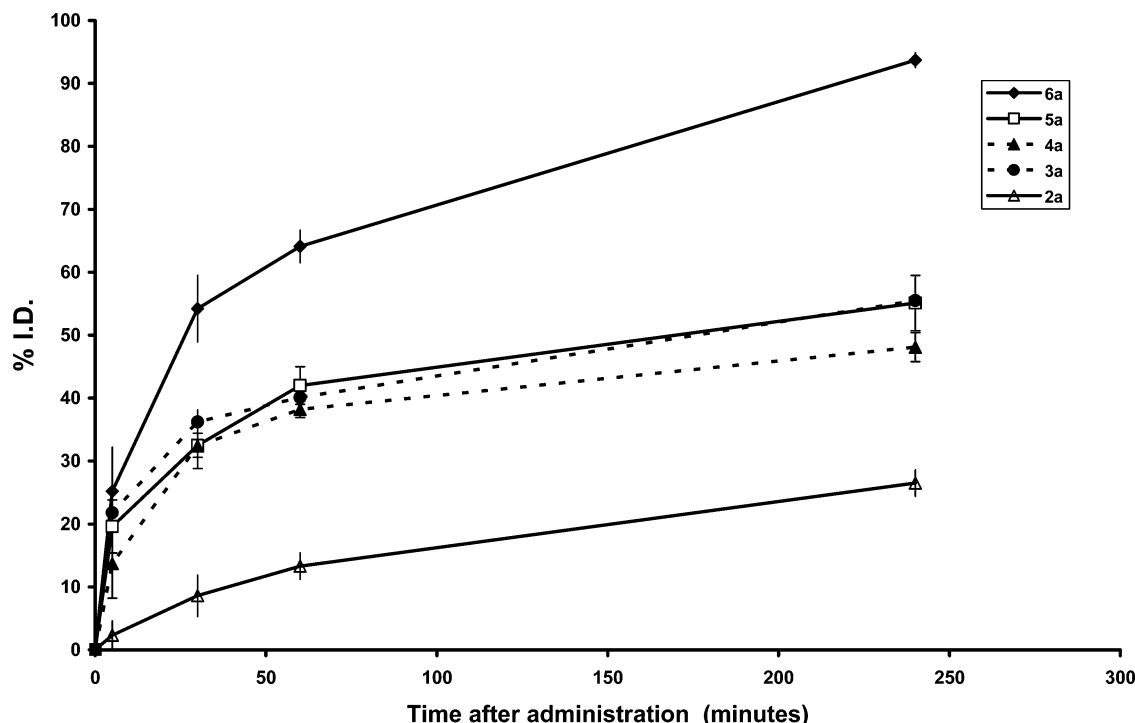
Figure 2. Histogram (% ID/g) for complexes 2a–6a in CD-1 Charles River, as a function of time after IV administration.

Table 2. Biodistribution (% ID/g) of <sup>99m</sup>TcComplexes 2a–6a in CD/1 Charles River, 4 h after IV Administration

organ	2a	3a	4a	5a	6a
blood	0.5 ± 0.1	1.0 ± 0.2	0.5 ± 0.2	0.10 ± 0.01	0.13 ± 0.01
liver	7.3 ± 1.8	2.3 ± 0.4	3.3 ± 0.6	1.8 ± 0.2	0.4 ± 0.1
intestine	12.8 ± 2.8	13.7 ± 3.5	16.9 ± 2.2	13.2 ± 1.6	0.7 ± 0.3
spleen	2.1 ± 0.5	0.47 ± 0.09	0.4 ± 0.1	0.11 ± 0.04	0.07 ± 0.01
pancreas	1.8 ± 0.1	1.9 ± 0.4	2.0 ± 0.3	2.0 ± 0.2	0.06 ± 0.01
heart	2.1 ± 0.3	0.9 ± 0.2	1.0 ± 0.2	0.35 ± 0.05	0.06 ± 0.02
lung	0.8 ± 0.1	0.59 ± 0.08	0.7 ± 0.1	0.5 ± 0.1	0.09 ± 0.03
kidney	11.0 ± 3.4	1.8 ± 0.2	2.5 ± 0.5	1.6 ± 0.1	2.2 ± 0.4
muscle	0.7 ± 0.1	0.15 ± 0.03	0.29 ± 0.04	0.08 ± 0.02	0.02 ± 0.01
bone	0.5 ± 0.1	0.15 ± 0.02	0.24 ± 0.01	0.2 ± 0.1	0.04 ± 0.01
stomach	2.4 ± 0.4	1.4 ± 0.4	2.4 ± 0.1	1.5 ± 0.2	0.08 ± 0.01

ent complexes are related to the clearance from tissues as well as to the rate of overall excretion. The highest retention of activity in all organs was observed for complex 2a with most of the radioactivity retained in

kidneys, liver, and intestines. The rate of injected dose cleared via the liver into the intestines is also slightly slower for 2a, and consequently the total radioactivity excretion from whole animal body is significantly slower



**Figure 3.** Total excretion for the tricarbonyl complexes **2a–6a**.

than for the other complexes (Figure 3). Complexes **3a–5a** have similar biological behavior in mice with few significant differences in their pharmacokinetics. As compared to these complexes, **6a** shows a faster clearance from the main organs and the total radioactivity excretion was relatively enhanced while the hepatic retention was reduced. Despite knowing that parameters other than lipo(hydro)philicity can affect the biodistribution profile, the predominant route of excretion, the urinary tract, seems to correlate with the  $\log P_{o/w}$  values found for the complexes (Table 1). The highest hepatic retention was found for **2a**, which has a  $\log P_{o/w}$  value of 0.87, while for **6a** which has a  $\log P_{o/w}$  value of  $-2.35$  was observed a more rapid clearance and total excretion. The high hydrophilicity of **6a** and the rapid total radioactivity excretion may be related to the presence of the carboxylate group introduced in the 4-position of the pyrazolyl ring.

**Bifunctional Pyrazolyl Chelators for the Labeling of Peptides.** Taking into account the in vitro stability, lipophilicity, and biological profile of the building blocks previously described, we consider that all of the ligands, except for ligand **2a**, are very promising for labeling biologically active peptides. To have better insight into this aspect, we have decided to evaluate the possibility of preparing bifunctional chelators based on the **L<sup>2</sup>** and **L<sup>4</sup>** lead structures. By choosing these ligand frameworks, we also took into account that **L<sup>2</sup>** and **L<sup>4</sup>** allowed the synthesis of the <sup>99m</sup>Tc-building blocks with high specific activity (Table 1), being very similar in terms of biological profile and only slightly different in terms of molecular weight and lipophilicity.

The synthesis of the bifunctional pyrazolyl chelators involved the selective BOC protection of the primary amine functions of **L<sup>2</sup>** and **L<sup>4</sup>**, followed by alkylation of the secondary amine with ethyl 4-bromobutyrate. 3,5-Me<sub>2</sub>-pz(CH<sub>2</sub>)<sub>2</sub>N((CH<sub>2</sub>)<sub>3</sub>COOH)(CH<sub>2</sub>)<sub>2</sub>NH<sub>2</sub> (**L<sup>6</sup>**) and pz(CH<sub>2</sub>)<sub>2</sub>N((CH<sub>2</sub>)<sub>3</sub>COOH)(CH<sub>2</sub>)<sub>2</sub>NH<sub>2</sub> (**L<sup>7</sup>**), having a carboxylate group suitable for conjugation of tumor-seeking peptides, were finally obtained as yellow oils, after ester

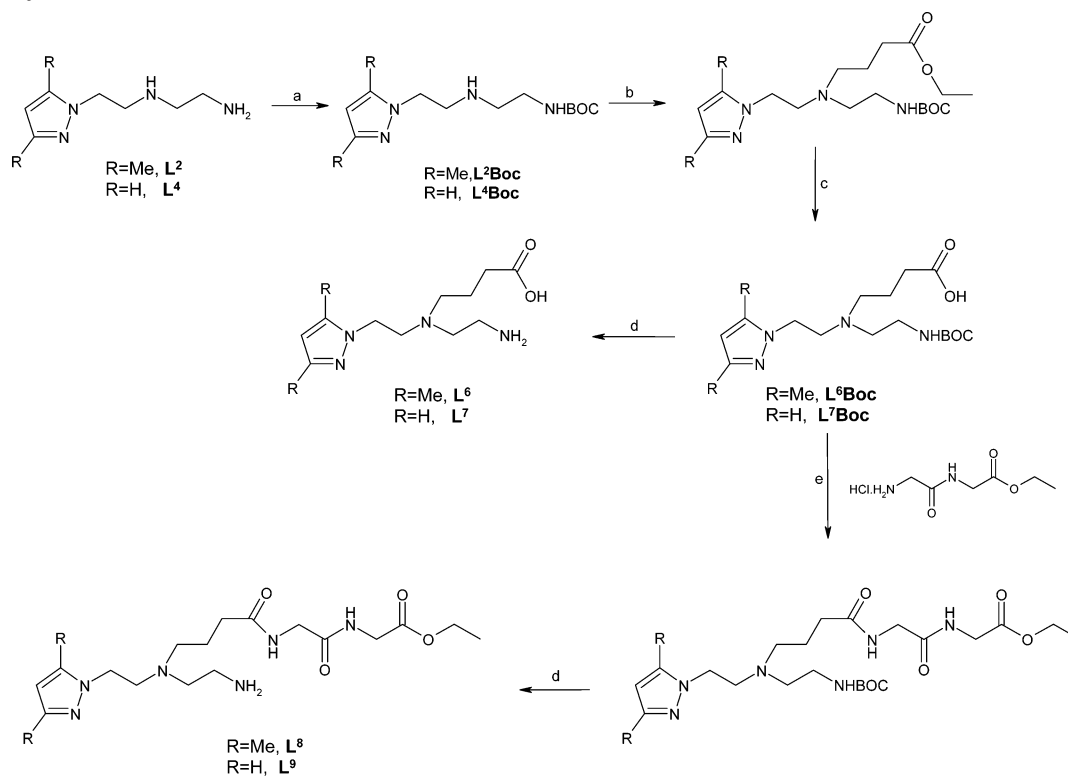
hydrolysis and removal of the BOC protecting group (Scheme 2).

Considering that the introduction of a pendant carboxylate group could modify the coordination mode of the pyrazolyl derivatives, we decided to study reactions of (NEt<sub>4</sub>)<sub>2</sub>[ReBr<sub>3</sub>(CO)<sub>3</sub>] (**1**) with **L<sup>6</sup>** and **L<sup>7</sup>**. Both ligands react promptly with **1**, leading to the formation of complexes [Re(CO)<sub>3</sub>(κ<sup>3</sup>-L)] (L = **L<sup>6</sup>** (**7**), **L<sup>7</sup>** (**8**)). On the basis of the splitting and chemical shifts of the <sup>1</sup>H and <sup>13</sup>C NMR resonances (vide experimental data), we concluded that in **7** and **8** the chelators **L<sup>6</sup>** and **L<sup>7</sup>** act as tridentate through the nitrogen atoms, similarly to the coordination mode found for the parent ligands **L<sup>2</sup>** and **L<sup>4</sup>** in complexes **3** and **5**, respectively (Scheme 1). These results prompted the coupling of the **L<sup>6</sup>** and **L<sup>7</sup>** to glycylglycine used as a peptide model, to prove the utility of these bifunctional chelators for labeling biologically relevant molecules.

The coupling of the dipeptide to **L<sup>6</sup>** and **L<sup>7</sup>** was achieved by reacting **L<sup>6</sup>-BOC** or **L<sup>7</sup>-BOC** with ethyl glycylglycine ester in the presence of HBTU and NEt<sub>3</sub>, followed by deprotection of the primary amine and hydrolysis of the ester (Scheme 2). The coordination capability of the resulting functionalized ligands **L<sup>8</sup>** and **L<sup>9</sup>** toward the *fac*-[M(CO)<sub>3</sub>] (M = Re, <sup>99m</sup>Tc) moiety was evaluated by reacting these ligands with **1/1a** under aqueous conditions (Scheme 3). These reactions are accompanied by hydrolysis of the ester function of the glycylglycine fragment, and the complexes synthesized were *fac*-[M(CO)<sub>3</sub>(κ<sup>3</sup>-3,5-Me<sub>2</sub>-pz(CH<sub>2</sub>)<sub>2</sub>N(glygly)(CH<sub>2</sub>)<sub>2</sub>NH<sub>2</sub>)]<sup>+</sup> (**9/9a**) and *fac*-[M(CO)<sub>3</sub>(κ<sup>3</sup>-pz(CH<sub>2</sub>)<sub>2</sub>N(CH<sub>2</sub>)<sub>3</sub>(glygly)(CH<sub>2</sub>)<sub>2</sub>NH<sub>2</sub>)]<sup>+</sup> (**10/10a**) (M = Re, <sup>99m</sup>Tc) (Scheme 3).

Compound **9** was characterized by ES/MS, IR, <sup>1</sup>H, and <sup>13</sup>C NMR spectroscopy, while the formulation of **10** was only established by ES/MS. The <sup>99m</sup>Tc complexes were characterized by comparing their radioactive traces on the HPLC with the UV traces of the analytically pure Re analogues.

The <sup>99m</sup>Tc-complexes **9a** and **10a** were obtained in high radiochemical purity, using final ligand concentrations

Scheme 2.<sup>a</sup> Synthesis of  $L^6$ – $L^9$ 

<sup>a</sup> (a) BOC-ON, THF/DMF, 0 °C, 2 h; (b) ethyl 1-bromobutyrate/ $\text{K}_2\text{CO}_3/\text{KI}/\text{CH}_3\text{CN}$ ; (c) NaOH,  $\text{H}_2\text{O}$ , THF, reflux, o.n.; (d) TFA,  $\text{CH}_2\text{Cl}_2$ , room temperature, 1 h; (e) HBTU,  $\text{NEt}_3$ ,  $\text{CH}_3\text{CN}$ , room temperature, 4 h.

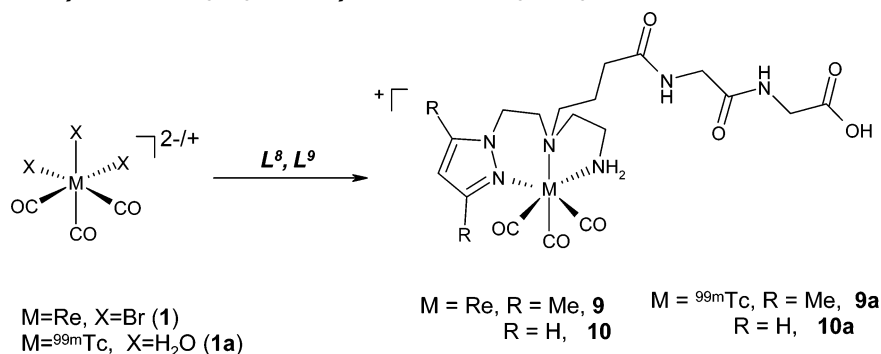
Scheme 3. Reactions of  $\text{fac-}[\text{Re}(\text{CO})_3\text{Br}_3]^{2-}$  and  $\text{fac-}[\text{}^{99\text{m}}\text{Tc}(\text{H}_2\text{O})_3(\text{CO})_3]^+$  with  $L^8$  and  $L^9$ 

Table 3. Experimental Conditions for the Synthesis of Complexes **9a** and **10a** and Characteristics of the Complexes

complex	yield [%]	$c$ [M]	$t$ [min]	$T$ (°C)	RT (min) <sup>a</sup>	$\log P_{o/w} \pm s$
<b>9a</b> ( $L^8$ )	$\geq 95$	$(3-5) \times 10^{-5}$	60/30	100	19.2 (18.7) <sup>b</sup>	$-1.12 \pm 0.20$
<b>10a</b> ( $L^9$ )	$\geq 90$	$(3-5) \times 10^{-5}$	60/30	100	17.2 (16.8) <sup>b</sup>	$-2.11 \pm 0.02$

<sup>a</sup> The values in parentheses are for the rhenium complexes. <sup>b</sup> Nucleosil 250-4 100-10 C18 columns, flow of 1 mL/min.

in the  $(3-5) \times 10^{-5}$  M range (Table 3), which are not significantly higher than the concentrations of  $L^1$  and  $L^4$  used to prepare the parent building blocks **3a** and **5a**. Hence, the attachment of the pendant arm at the central nitrogen does not strongly affect the coordination capability of these pyrazolyl-based chelators. Consistently, as complexes **3a** and **5a**, the glycyglycine functionalized complexes **9a** and **10a** also displayed a high robustness in cysteine and histidine challenge experiments.

In Table 4 are presented the biodistribution data of complexes **9a** and **10a** in CD-1 mice as percentage of injected dose per gram of organ, as well as the total radioactivity excretion as a function of time.

These results clearly indicate a biodistribution and pharmacokinetics for the glycyglycine functionalized

complexes that are comparable to those found for building blocks **3a** and **5a**. However, for **9a** and **10a**, the enhanced urinary excretion, due to a lower retention of radioactivity in the kidneys over time, increased the percentage of overall excretion. To verify the in vivo stability of complexes **9a** and **10a**, serum, liver homogenate, and urine of the murines were also analyzed by radiometric HPLC. The murine serum, isolated from blood collected 30 min after i.v. administration, shows no pertechnetate, and more than 98% of the radioactivity could be assigned to complexes **9a** and **10a**. Furthermore, HPLC analysis of liver homogenate, from mice sacrificed 1 h after administration, also revealed that more than 98% of the radioactivity could be assigned to the  ${}^{99\text{m}}\text{Tc}$ -tricarbonyl complexes **9a** and **10a**, indicating their resistance to

**Table 4. Biodistribution (% ID/g) of  $^{99m}\text{Tc}$  Complexes 9a and 10a in CD/1 Charles River, as a Function of Time after IV Administration**

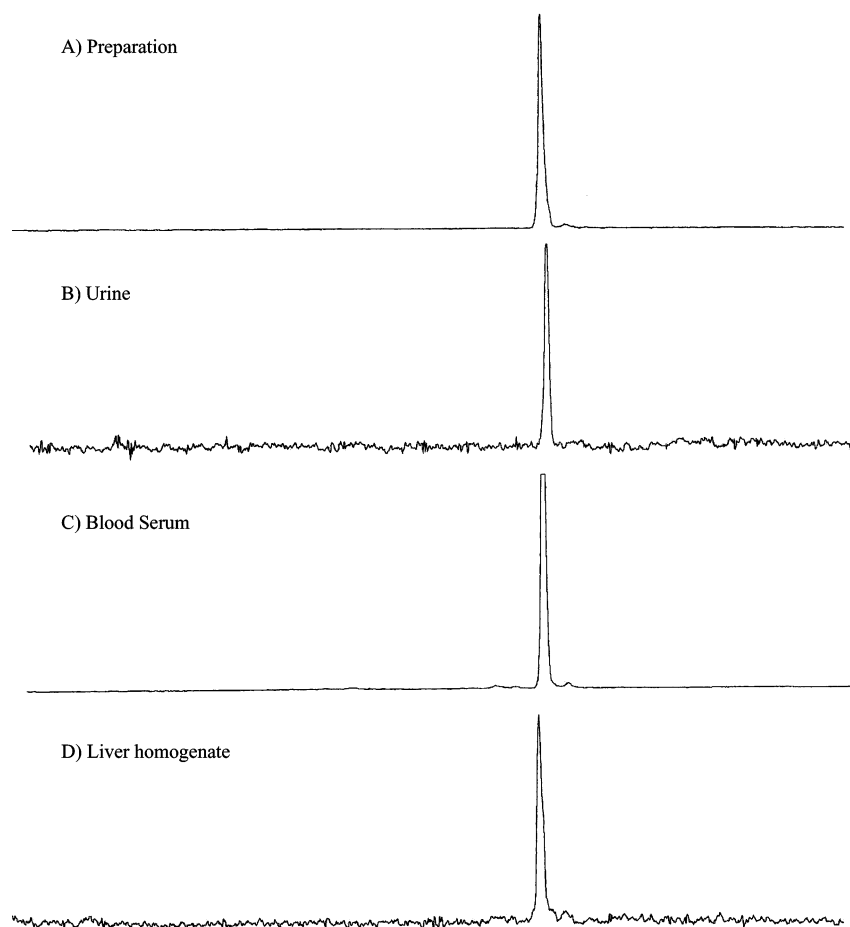
organ	9a				10a			
	5 min	30 min	60 min	240 min	5 min	30 min	60 min	240 min
blood	9.1 ± 1.3	1.7 ± 0.2	0.88 ± 0.04	0.39 ± 0.03	5.0 ± 0.9	0.9 ± 0.1	0.45 ± 0.06	0.06 ± 0.02
liver	17.1 ± 0.6	10.2 ± 1.2	4.8 ± 1.3	5.4 ± 0.8	19.8 ± 2.5	22.6 ± 3.1	14.7 ± 2.7	2.9 ± 0.8
intestine	2.7 ± 0.4	11.0 ± 2.1	7.7 ± 1.2	9.6 ± 1.7	1.7 ± 0.2	4.5 ± 0.9	7.5 ± 2.2	14.2 ± 2.0
spleen	2.5 ± 0.8	1.2 ± 0.2	0.5 ± 0.2	1.8 ± 0.4	0.7 ± 0.1	0.14 ± 0.04	0.08 ± 0.01	0.03 ± 0.02
pancreas	1.1 ± 0.1	0.4 ± 0.1	0.24 ± 0.04	0.16 ± 0.01	1.0 ± 0.1	0.3 ± 0.1	0.3 ± 0.1	0.08 ± 0.03
heart	1.8 ± 0.2	0.4 ± 0.1	0.24 ± 0.02	0.25 ± 0.04	1.1 ± 0.2	0.25 ± 0.06	0.12 ± 0.02	0.03 ± 0.00
lung	12.3 ± 0.9	1.5 ± 0.1	0.94 ± 0.05	3.8 ± 0.9	2.1 ± 0.3	0.49 ± 0.04	0.19 ± 0.05	0.05 ± 0.02
kidney	9.6 ± 0.4	2.9 ± 0.5	1.7 ± 0.2	1.0 ± 0.1	11.2 ± 1.3	3.1 ± 0.9	1.2 ± 0.2	0.26 ± 0.03
muscle	1.2 ± 0.2	0.25 ± 0.06	0.14 ± 0.03	0.08 ± 0.01	1.1 ± 0.3	0.18 ± 0.05	0.08 ± 0.01	0.02 ± 0.01
bone	1.6 ± 0.2	0.30 ± 0.07	0.15 ± 0.01	0.14 ± 0.01	1.2 ± 0.3	0.21 ± 0.04	0.08 ± 0.01	0.05 ± 0.03
stomach	1.0 ± 0.5	1.2 ± 0.3	0.4 ± 0.2	0.4 ± 0.1	0.7 ± 0.6	0.6 ± 0.3	0.7 ± 0.2	0.3 ± 0.1
excretion (% I.D./organ)	16.9 ± 1.4	46.8 ± 5.8	57.7 ± 2.2	59.5 ± 2.6	24.6 ± 3.9	40.2 ± 6.1	55.2 ± 9.6	63.1 ± 6.0

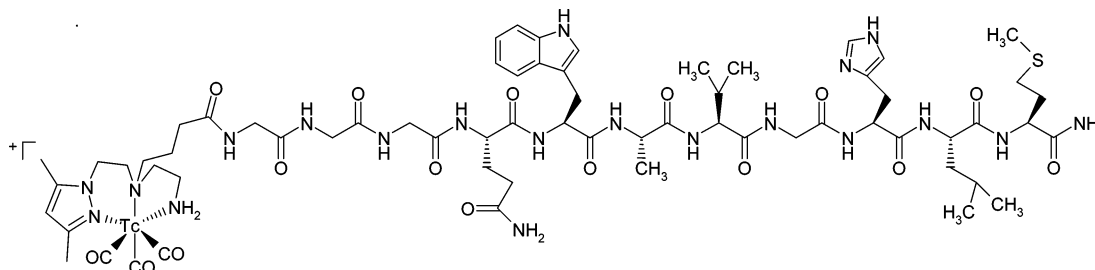
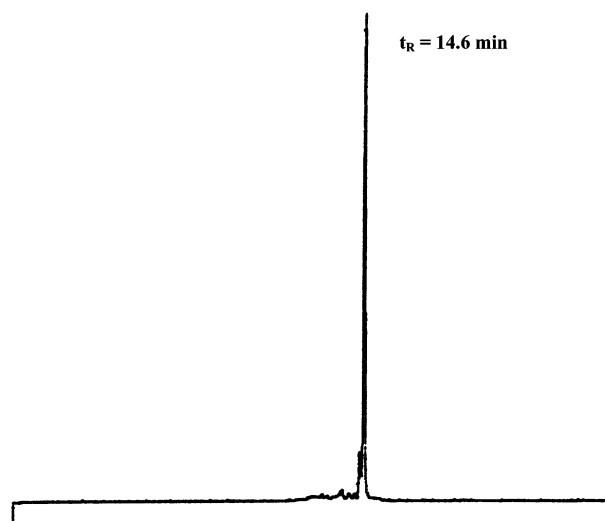
metabolic degradation. Analysis of urine collected at sacrifice time demonstrated again high *in vivo* stability of the complexes, because no metabolites could be detected. As an example, the HPLC chromatograms of biological samples collected from mice injected with **9a** are shown in Figure 4. The resistance to metabolic degradation in blood and liver, an organ rich in enzymes such as peptidases, and the excretion of the  $^{99m}\text{Tc}$  tricarbonyl complexes intact into the urine demonstrate their high *in vivo* robustness.

To further demonstrate the utility of this family of bifunctional chelators in synthesizing receptor-avid peptide pyrazolyl conjugates, a GRP receptor-specific peptide (G-G-G-Q-W-A-V-G-H-L-M-NH<sub>2</sub>) was chosen for coupling to **L<sup>6</sup>**. The new conjugate was synthesized by SPPS and

characterized by electrospray ionization mass spectrometry. The radiolabeled peptide conjugate [ $^{99m}\text{Tc}(\text{CO})_3$ -**L<sup>6</sup>**-(GGG)-Bombesin(7-14)NH<sub>2</sub>] (**11a**) was obtained in high yield ( $\geq 95\%$ ) upon addition of 100  $\mu\text{L}$  of a solution of the conjugate ( $(3-5) \times 10^{-5}$  M) to a vial containing 900  $\mu\text{L}$  of the precursor [ $^{99m}\text{Tc}(\text{CO})_3(\text{H}_2\text{O})_3$ ], with heating (Figure 5). Radiochemical yields of the new  $^{99m}\text{Tc}$ -conjugates were monitored by RP-HPLC. The chromatographic profile of metalated conjugate is shown in Figure 6. The chromatogram displays a single peak with a retention time of 14.6 min. This conjugate is stable in aqueous solution for time periods of  $\geq 24$  h.

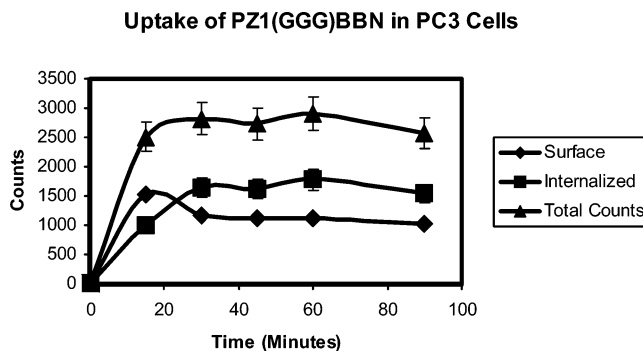
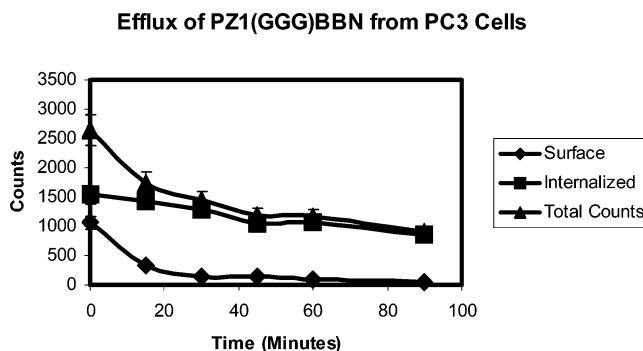
Competitive binding displacement studies of [**L<sup>6</sup>**-(GGG)-Bombesin(7-14)NH<sub>2</sub>] demonstrated an IC<sub>50</sub> value of  $0.7 \pm 0.2$  nM. This value is very much comparable to

**Figure 4.** HPLC chromatogram for complex **10a**: (A) preparation, (B) urine, (C) blood serum, and (D) liver homogenate.


**Figure 5.** Metalated BBN analogue (**11a**).

**Figure 6.** HPLC elution profile of the metalated BBN analogue [ $^{99m}\text{Tc}(\text{CO})_3\text{-L}^6\text{-(GGG)-Bombesin(7-14)NH}_2$ ] (**11a**) ( $t_R$ , 14.6 min).

those previously reported for conjugates of this type (33–36).

Figure 7 summarizes the results of studies to assess the degree of uptake (internalization) of the new conjugate in PC-3 cells. At 90 min postincubation, the amount of internalized activity is  $\sim 60\%$  of the total activity administered. These data are considerably lower when compared to other conjugates of this type (35, 36). Figure 8 summarizes the results of studies to assess the degree of trapping (efflux) of the [ $^{99m}\text{Tc}(\text{CO})_3\text{-L}^6\text{-(GGG)-Bombesin(7-14)NH}_2$ ] (**11a**) in PC-3 cells. The total  $^{99m}\text{Tc}$  activity associated with the cells after the 45 min incubation was measured following washing of the cells with the pH 7.4 incubation media. After washing these cells with the pH 2.5 buffer to remove surface-bound  $^{99m}\text{Tc}$  activity, approximately 60% remained trapped by the cells. Results of measurements at 15, 30, 45, 60, and 90 min show that


**Figure 7.** Internalization of [ $^{99m}\text{Tc}(\text{CO})_3\text{-L}^6\text{-(GGG)-Bombesin(7-14)NH}_2$ ] (**11a**) in human prostate (PC-3) cancerous cells.

**Figure 8.** Efflux of [ $^{99m}\text{Tc}(\text{CO})_3\text{-L}^6\text{-(GGG)-Bombesin(7-14)NH}_2$ ] (**11a**) in human prostate (PC-3) cancerous cells.

radioactivity does remain trapped by the cells, with approximately 45% of the  $^{99m}\text{Tc}$ -activity associated with the cells at  $t = 0$  remaining residualized at 90 min. Thus, at 90 min, approximately 66% of the activity remains residualized when normalized to the 60% trapped in the cells at  $t = 0$ . Efflux of this conjugate from PC-3 prostate tumor cells is comparable to other  $^{99m}\text{Tc}(\text{I})$ -conjugates of this type (35, 36). The introduction of the pyrazolyl ligand

**Table 5.** Biodistribution of [ $^{99m}\text{Tc}(\text{CO})_3\text{-L}^6\text{-(GGG)-Bombesin(7-14)NH}_2$ ] (**11a**) in CF-1 Normal Mice as a Function of Time after IV Administration

organ	% ID/organ			% ID/g organ		
	1 h	4 h	24 h	1 h	4 h	24 h
blood	1.35 ± 0.06	0.76 ± 0.20	0.23 ± 0.07	0.80 ± 0.04	0.45 ± 0.12	0.14 ± 0.04
liver	5.73 ± 1.10	2.43 ± 0.79	1.88 ± 0.27	3.77 ± 0.80	1.64 ± 0.55	1.17 ± 0.11
intestine	24.3 ± 3.92	18.3 ± 6.62	0.49 ± 0.05	16.2 ± 1.70	19.0 ± 6.54	0.38 ± 0.04
spleen	0.05 ± 0.02	0.02 ± 0.01	0.01 ± 0.00	1.17 ± 1.72	0.34 ± 0.30	0.17 ± 0.05
pancreas	1.05 ± 0.20	0.09 ± 0.03	0.03 ± 0.01	5.80 ± 0.87	0.46 ± 0.01	0.15 ± 0.04
heart	0.05 ± 0.01	0.03 ± 0.01	0.02 ± 0.01	0.42 ± 0.14	0.23 ± 0.12	0.13 ± 0.05
lung	0.12 ± 0.01	0.10 ± 0.03	0.05 ± 0.01	0.54 ± 0.11	0.54 ± 0.31	0.20 ± 0.03
kidney	0.87 ± 0.09	0.59 ± 0.18	0.34 ± 0.03	2.20 ± 0.30	1.77 ± 0.57	0.91 ± 0.17
muscle	0.02 ± 0.00	0.01 ± 0.01	0.01 ± 0.01	0.10 ± 0.02	0.14 ± 0.16	0.06 ± 0.03
bone	0.03 ± 0.00	0.01 ± 0.01	0.01 ± 0.01	0.31 ± 0.14	0.25 ± 0.22	0.35 ± 0.50
stomach	0.30 ± 0.12	0.13 ± 0.04	0.09 ± 0.05	0.72 ± 0.26	0.21 ± 0.14	0.12 ± 0.07
carcass	5.24 ± 0.79	4.15 ± 2.40	1.45 ± 0.29	5.24 ± 0.79	5.24 ± 0.79	5.24 ± 0.79
bladder	0.06 ± 0.03	0.01 ± 0.01	0.01 ± 0.00	3.32 ± 1.47	0.53 ± 0.50	0.29 ± 0.22
urine	60.7 ± 2.94	73.3 ± 9.27	67.3 ± 7.28			

onto BBN[7-14]NH<sub>2</sub> has little or no effect on the efflux properties of the <sup>99m</sup>Tc-conjugate in GRP receptor-specific PC-3 cells as this new conjugate demonstrates uptake comparable to other <sup>99m</sup>Tc(I)-conjugates of this type (35, 36).

Table 5 summarizes the results of the biodistribution studies in normal CF-1 mice at 1 h postintravenous injection for the [<sup>99m</sup>Tc(CO)<sub>3</sub>-L<sup>6</sup>-(GGG)-Bombesin(7-14)NH<sub>2</sub>] conjugate. The conjugate was surprisingly hydrophilic with 71.9 ± 2.49% ID clearing via the renal-urinary pathway at 4 h p.i. The remainder of the radioactivity was cleared via the hepatobiliary pathway. There is no significant uptake or retention in the stomach, indicating that there is minimal, if any, in vivo dissociation of <sup>99m</sup>Tc from the pyrazolyl ligand to produce <sup>99m</sup>TcO<sub>4</sub><sup>-</sup>. Pancreatic tissue expresses the GRPr in high density. Therefore, the accumulation of <sup>99m</sup>Tc-activity in pancreatic tissue reflects the ability of these derivatives to target GRP receptor-expressing cells in vivo. Receptor-mediated pancreatic uptake of this <sup>99m</sup>Tc-conjugate was noticeably lower (i.e., 5.8 ± 0.87% ID/g at 1 h p.i.) when compared to other BBN conjugates designed and developed in our laboratory. This is presumably due to an increased rate of clearance from serum into the hepatobiliary system as compared to other more hydrophilic conjugates of similar structure (33–36). Kidney retention for the <sup>99m</sup>Tc-conjugate was found to be ~2% ID/g. Blocking studies in which high levels of cold BBN[1-14] was administered 30 min prior to the <sup>99m</sup>Tc-ligands reduced the % ID/g uptake/retention in the pancreas at 1 h p.i. significantly, demonstrating the in vivo receptor specificity of this analogue for GRP-receptor expressing cells (data not shown).

## CONCLUSION

The pyrazolyl-based chelators L<sup>1</sup>–L<sup>5</sup> react with (NEt<sub>4</sub>)<sub>2</sub>-[ReBr<sub>3</sub>(CO)<sub>3</sub>] (1) and [<sup>99m</sup>Tc(H<sub>2</sub>O)<sub>3</sub>(CO)<sub>3</sub>]<sup>+</sup> (1a) forming well-defined complexes of the type [M(CO)<sub>3</sub>(k<sup>3</sup>-L)]<sup>+</sup>. The <sup>99m</sup>Tc complexes are obtained in high yield, with high radiochemical purity, and are stable against cysteine and histidine exchange reactions. The biological profile and pharmacokinetics of these building blocks indicate that they were rapidly cleared from blood and other main organs into urine, mainly the renal-urinary pathway, with a small portion retained in the hepatobiliary tract. Most of these ligands can be functionalized through the primary or secondary amine as well as through the pyrazolyl ring. In this report, we have explored functionalization through the secondary amine. We have shown that the introduction of a pendant carboxylate arm on L<sup>2</sup> and L<sup>4</sup> does not change the coordination mode of the final bifunctional chelators. Furthermore, coupling of this ligand to a small peptide such as BBN(7-14)NH<sub>2</sub> does not change the high in vitro and in vivo stability of the metalated conjugates. This important requirement together with the favorable tissue distribution profile of the complexes/conjugate (i.e., rapid clearance from non-target tissue, rapid urinary excretion, and low retention of radioactivity in the kidneys) are quite attractive features of these pyrazolyl derivatives. In summary, these results can be seen as proof-of-principle of the utility of tridentate and asymmetric pyrazolyl-based ligands as bifunctional chelators for labeling tumor-seeking peptides with the *fac*-[<sup>99m</sup>Tc(CO)<sub>3</sub>]<sup>+</sup> moiety. Moreover, the characteristics of the ligands are expected to allow a fine-tuning of the biological properties of the labeled tumor-seeking peptides.

## ACKNOWLEDGMENT

We thank Mallinckrodt-Tyco Inc. for financial support. S.A. thanks Fundação para a Ciência e Tecnologia for a Ph.D. grant (BD/3052/2000). We would also like to acknowledge the research group of Dr. Timothy J. Hoffman at the Harry S. Truman Memorial Veterans' Hospital and the University of Missouri–Columbia for contributing effort toward the biodistribution analysis of the bombesin conjugates.

## LITERATURE CITED

- (1) Hom, R. K., and Katzenellenbogen, J. A. (1997) Technetium-99m.-Labeled Receptor-Specific Small-Molecule Radiopharmaceuticals: Recent Development and Encouraging Results *Nucl. Med. Biol.* 24, 485–498.
- (2) Dilworth, J. R., and Parrott, S. J. (1998) The Biomedical Chemistry of Technetium and Rhenium. *Chem. Soc. Rev.* 27, 43.
- (3) Jurisson, S. S., and Lydon, J. D. (1999) Potential technetium small molecules radiopharmaceuticals. *Chem. Rev.* 99, 2205–2218.
- (4) Liu, S., and Edwards, D. S. (1999) <sup>99m</sup>Tc-labeled small peptides as diagnostic radiopharmaceuticals. *Chem. Rev.* 99, 2235–2268.
- (5) Heppeler, A., Froidevaux, S., Eberle, A. N., and Maecke, H. R. (2000) Receptor Targeting for Tumor Localisation and Therapy with Radiopeptides. *Curr. Med. Chem.* 7, 971–994.
- (6) Behr, T. M., Gotthardt, M., Barth, A., and Béhé, M. (2001) Imaging tumors with peptide-based radioligands. *Q. J. Nucl. Med.* 45, 189–200.
- (7) Okarvi, S. M. (2004) Peptide-Based Radiopharmaceuticals: Future Tools for Diagnostic Imaging of Cancers and Other Diseases. *Med. Res. Rev.* 24, 357–397.
- (8) Kwekkeboom, D., Krenning, E. P., and de Jong, M. (2000) Peptide Receptor Imaging and Therapy. *J. Nucl. Med.* 41, 1704–1713.
- (9) Alberto, R., Schibli, R., Egli, A., Schubiger, P. A., Herrmann, W. A., Artus, G., Abram, U., and Kaden, T. A. (1995) Metal-carbonyl syntheses. Low-pressure carbonylation of MOCl<sub>4</sub><sup>-</sup> and MO<sub>4</sub><sup>-</sup>-the technetium(I) and rhenium(I) complexes [NEt<sub>4</sub>]<sub>2</sub>-[MCl<sub>3</sub>(CO)<sub>3</sub>]. *J. Organomet. Chem.* 493, 119–127.
- (10) Alberto, R., Schibli, R., Egli, A., Schubiger, P. A., Abram, U., and Kaden, T. A. (1998) A novel organometallic aqua complex of technetium for the labeling of biomolecules: synthesis of [<sup>99m</sup>Tc(H<sub>2</sub>O)<sub>3</sub>(CO)<sub>3</sub>]<sup>+</sup> from [<sup>99m</sup>TcO<sub>4</sub>]<sup>-</sup> in aqueous solution and its reaction with a bifunctional ligand. *J. Am. Chem. Soc.* 120, 7987–7988.
- (11) Metzler-Nolte, N. (2001) Labeling of Biomolecules for Medicinal Applications – Bioorganometallic Chemistry at Its Best. *Angew. Chem., Int. Ed.* 40, 1040–1043.
- (12) Schibli, R., La Bella, R., Alberto, R., Garcia-Garayoa, E., Ortner, K., Abram, U., and Schubiger, P. A. (2000) Influence of the Denticity of Ligand Systems on the in Vitro and in Vivo Behaviour of <sup>99m</sup>Tc(I) Tricarbonyl Complexes: A Hint for the Future Functionalization of Biomolecules. *Bioconjugate Chem.* 11, 345–351.
- (13) Garcia, R., Paulo, A., Domingos, A., Santos, I., Ortner, K., and Alberto, R., (2000) Re and Tc Complexes Containing B–H...M Agostic Interactions as Building Blocks for the Design of Radiopharmaceuticals. *J. Am. Chem. Soc.* 122, 11240–11241.
- (14) Wald, J., Alberto, R., Ortner, K., and Candraia, L. (2001) Aqueous One-Pot Synthesis of Derivatized Cyclopentadienyl – Tricarbonyl Complexes of <sup>99m</sup>Tc with an In Situ CO Source: Application to a Serotonergic Receptor Ligand. *Angew. Chem., Int. Ed.* 40, 3062–3066.
- (15) Correia, J. D. G., Domingos, A., Santos, I., Alberto, R., and Ortner, K. (2001) Re Tricarbonyl Complexes with Ligands Containing P, N, N and P, N, O Donor Atom Set: Synthesis and Structural Characterization. *Inorg. Chem.* 40, 5147–5151.
- (16) Garcia, R., Paulo, A., Domingos, A., and Santos, I. (2001) Rhenium(I) Organometallic Complexes with Novel Bis(mercaptoimidazolyl)borates and with Hydrotris(mercaptoimid-

- azolyl)borate: Chemical and Structural Studies. *J. Organomet. Chem.* 632, 41.
- (17) Sogbein, O. O., Merdy, P., Morel, P., and Valliant, J. F. (2004) Preparation of Re(I)- and  $^{99m}\text{Tc}$ (I)-Metallo-carboranes in Water under Weakly Basic Reaction Conditions. *Inorg. Chem.* 43, 3032–3034.
- (18) Bernard, J., Ortner, K., Spingler, B., Pietzsch, H.-J., and Alberto, R. (2003) Aqueous Synthesis of Derivatized Cyclopentadienyl Complexes of Technetium and Rhenium Directed toward Radiopharmaceutical Application. *Inorg. Chem.* 42, 1014–1022.
- (19) Pak, J. K., Benny, P., Spingler, B., Ortner, K., and Alberto, R. (2003)  $\text{N}^{\epsilon}$  Functionalization of Metal and Organic Protected L-Histidine for a Highly Efficient, Direct Labeling of Biomolecules with  $[\text{Tc}(\text{OH}_2)_3(\text{CO})_3]^+$ . *Chem.-Eur. J.* 9, 2053–2061.
- (20) Alves, S., Paulo, A., Correia, J. D. G., Domingos, A., and Santos, I. (2002) Coordination Capabilities of Pyrazolyl Containing Ligands Towards the *fac*- $[\text{Re}(\text{CO})_3]^+$  Moiety. *J. Chem. Soc., Dalton Trans.* 24, 4714–4719.
- (21) Vitor, R., Alves, S., Correia, J. D. G., Paulo, A., and Santos, I. (2004) Rhenium(I)- and Technetium(I) Tricarbonyl Complexes Anchored by Bifunctional Pyrazole-Diamine and Pyrazole-Dithioether Chelators. *J. Organomet. Chem.* 689, 4764–4774.
- (22) Alves, S., Paulo, A., Correia, J. D. G., Gano, L. A., and Santos, I. (2002) New Building Blocks for Labeling Peptides with the  $[\text{Re}(\text{CO})_3]^+$  Core. *Technetium, Rhenium and Other Metals in Chemistry and Nuclear Medicine 6* (Nicolini, M., Mazzi, U., Eds.) pp 139–142, SGEEditoriali, Padova.
- (23) Mahmoud, S., Staley, J., Taylor, J., Bogden, A., Moreau, J.-P., Coy, D., Avis, I., Cuttitta, F., Mulshine, J. L., and Moody, T. W. (1985)  $[\text{P}^{13,14}]$  Bombesin Analogues Inhibit Growth of Small Cell Lung Cancer In Vitro and In Vivo. *Life Sci.* 37, 105–113.
- (24) Qin, Y., Ertl, T., Cai, R.-Z., Halmos, G., and Schally, A. V. (1994) Inhibitory Effect of Bombesin Receptor Antagonist RC-3095 on the Growth of Human Pancreatic Cancer Cells In Vivo and In Vitro. *Cancer Res.* 54, 1035–1041.
- (25) Qin, Y., Ertl, T., Cai, R.-Z., Horvath, J. E., Groot, K., and Schally, A. V. (1995) Antagonists of Bombesin/Gastrin-releasing Peptide Inhibit Growth of SW-1990 Human Pancreatic Adenocarcinoma and Production of Cyclic AMP. *Int. J. Cancer* 63, 257–262.
- (26) Plonowski, A., Nagy, A., Schally, A. V., Sun, B., Groot, K., and Halmos, G. (2000) In Vivo Inhibition of PC-3 Human Androgen-independent Prostate Cancer by a Targeted Cytotoxic Bombesin Analogue, AN-215. *Int. J. Cancer* 88, 652–657.
- (27) Breeman, W. A. P., Hofland, L. J., De Jong, M., Bernard, B. F., Srinivasan, A., Kwekkeboom, D. J., Visser, T. J., and Krenning, E. P. (1999) Evaluation of Radiolabeled Bombesin Analogues for Receptor-targeted Scintigraphy and Radiotherapy. *Int. J. Cancer* 81, 658–665.
- (28) Breeman, W. A. P., De Jong, M., Bernard, B. F., Kwekkeboom, D. J., Srinivasan, A., van der Pluijm, M. E., Hofland, L. J., Visser, T. J., and Krenning, E. P. (1999) Pre-clinical Evaluation of  $[\text{In}^{111}\text{-DTPA-Pro}^1, \text{Tyr}^4]$  Bombesin, a New Radioligand for Bombesin-receptor Scintigraphy. *Int. J. Cancer* 83, 657–663.
- (29) Sorrel, T. N., and Malachowski, M. R. (1983) Mononuclear Three-Coordinate Copper (I) Complexes: Synthesis, Structure and Reaction with Carbon Monoxide. *Inorg. Chem.* 22, 1883–1887.
- (30) Haanstra, W. G., Driessen, W. L., Van Roon, M., Stoffels, A. L. E., and Reedijk, J. (1989) Unusual Chelating Properties of the Ligand 1,8-Bis (3, 5-dimethyl-1-pyrazolyl)-3,6-dithiaoctane (bddo). Crystal Structures of  $\text{Ni}(\text{bddo})(\text{NCS})_2$ ,  $\text{Zn}(\text{bddo})(\text{NCS})_2$  and  $\text{Cd}(\text{bddo})_2(\text{NCS})_4$ . *J. Chem. Soc., Dalton Trans.* 2309–2314.
- (31) Van Berkel, P. M., Driessen, W. L., Parlevliet, F. J., Reedijk, J., and Sherrington, D. C. (1997) Metal-uptake Behaviour by a Novel Pyrazole-Containing Ligand Immobilised on to Poly(Glycidylmethacrylate-co-trimethylolpropanetrimesic acid). *Eur. Polym. J.* 33, 129–135.
- (32) Lopez, P., Seipelt, G., Merkl, P., Sturz, L., Alvarez, J., Dolle, A., Zeidler, M. D., Cerdan, S., and Ballesteros, P. (1999) N-2-(Azol-1(2)yl)ethyliminodiacetic acids: A novel Series of Gd(III) Chelators as T2 Relaxation Agents for Magnetic Resonance Imaging. *Bioorg. Med. Chem.* 7, 517–527.
- (33) Smith, C. J., Gali, H., Sieckman, G. L., Hayes, D. L., Owen, N. K., Mazuru, D. G., Volkert, W. A., and Hoffman, T. J. (2003) Radiochemical Investigations of  $^{177}\text{Lu}$ -DOTA-8-Aoc-BBN[7–14] $\text{NH}_2$ : An In vitro/in vivo assessment of the Targeting Ability of this New Radiopharmaceutical for PC-3 Human Prostate Cancer Cells. *Nucl. Med. Biol.* 30, 101–109.
- (34) Smith, C. J., Volkert, W. A., and Hoffman, T. J. (2002) Gastrin Releasing Peptide (GRP) Receptor Targeted Radiopharmaceuticals: A Concise Update. *Nucl. Med. Biol.* 30, 861–868.
- (35) Smith, C. J., Sieckman, G. L., Owen, N. K., Hayes, D. L., Mazuru, D. L., Volkert, W. A., and Hoffman, T. J. (2003) Radiochemical Investigations of  $[\text{Re}(\text{H}_2\text{O})(\text{CO})_3\text{-Dpr-SSS-Bombesin}(7-14)\text{NH}_2]$ : Syntheses, Radiolabeling, and In Vitro/In Vivo Studies Where Dpr = Diaminopropionic Acid. *Anticancer Res.* 23, 63–70.
- (36) Smith, C. J., Sieckman, G. L., Owen, N. K., Hayes, D. L., Mazuru, D. G., Kannan, R., Volkert, W. A., and Hoffman, T. J. (2003) Radiochemical Investigations of GRP Receptor-specific  $[\text{Re}(\text{X})(\text{CO})_3\text{-Dpr-Ser-Ser-Ser-Gln-Trp-Ala-Val-Gly-His-Leu-Met-(NH}_2)]$  in PC-3, Tumor-bearing, Rodent Models: Syntheses, Radiolabeling, and In Vitro/In Vivo Studies Where Dpr = 2,3-Diaminopropionic acid and X =  $\text{H}_2\text{O}$  or  $\text{P}(\text{CH}_2\text{OH})_3$ . *Cancer Res.* 63, 4082–4088.